July 2015

Statistical Analyses of Historical Pipeline Incident Data with Application to the Risk Assessment of Onshore Natural Gas Transmission Pipelines

Chio Lam
The University of Western Ontario

Supervisor
Dr. Wenxing Zhou
The University of Western Ontario

Graduate Program in Civil and Environmental Engineering

A thesis submitted in partial fulfillment of the requirements for the degree in Master of Science

STATISTICAL ANALYSES OF HISTORICAL PIPELINE INCIDENT DATA WITH APPLICATION TO THE RISK ASSESSMENT OF ONSHORE NATURAL GAS TRANSMISSION PIPELINES

(Thesis format: Integrated Article)

by

Chio Lam

Graduate Program in Engineering Science
Department of Civil and Environmental Engineering

A thesis submitted in partial fulfillment
of the requirements for the degree of
Master of Engineering Science

The School of Graduate and Postdoctoral Studies
The University of Western Ontario
London, Ontario, Canada

Abstract

Statistical analyses of the pipe-related incident data for onshore gas transmission pipelines between 2002 and 2013 collected by the Pipeline and Hazardous Material Safety Administration (PHMSA) of the United States Department of Transportation (DOT) are conducted. It is found that the total length of the onshore gas transmission pipelines in the US is approximately 480,000 km as of 2013. The third-party interference, external corrosion, material failure and internal corrosion are the leading causes for the pipe-related incidents, responsible for over 75% of the total incidents between 2002 and 2013. Based on the pipeline mileage and incident data, the average rate of rupture incidents over the 12-year period between 2002 and 2013 is calculated to be 3.1×10^{-5} per km per year. Furthermore, external corrosion is found to be the leading cause for rupture incidents, with a corresponding rupture rate of 1.0×10^{-5} per km per year.

A log-logistic model is developed to evaluate the probability of ignition (POI) given a rupture of an onshore gas transmission pipeline using the maximum likelihood method based on a total of 188 rupture incidents between 2002 and 2014 collected from the PHMSA pipeline incident database. The product of the pipeline internal pressure at the time of incident and outside diameter squared is observed to be strongly correlated to POI while the location class of the pipeline is not, and thus the former is adopted as the sole predictor in the model. The 95% confidence interval is evaluated, and for practical engineering use, the 95% upper confidence bound is tabulated in a look-up table. The proposed model is further validated using an independent dataset reported in the literature.

The quantitative risk assessment of a hypothetical onshore gas transmission pipelines is illustrated by incorporating the statistics of the pipeline rupture incidents and POI model obtained in the present study. The thermal radiation hazards resulting from an ignited rupture of the pipeline are quantified using the well-known C-FER model. The heat intensity thresholds leading to fatality and injury for both the outdoor and indoor

exposure conditions are selected from the literature. The societal risk is then evaluated in terms of the expected number of casualties and *F-N* curve for the population located in the vicinity of the pipeline, whereas the individual risk is calculated as the annual probability of casualty of a specific individual located in the vicinity of the pipeline. The *F-N* curve is evaluated for each one kilometer section of the pipeline such that the section corresponding to the most critical *F-N* curve is identified.

Keywords

Onshore gas transmission pipeline; Pipeline incident; Rupture; Probability of ignition; Maximum likelihood method; Quantitative risk assessment; Societal risk, and Individual risk

Dedication

To my parents and grandparents

Acknowledgments

First of all, I would like to express my greatest gratitude to Dr. Wenxing Zhou for his unfailing support, help, guidance and encouragement with his profound knowledge and vast enthusiasm through the completion of my master program. I have benefited and learnt a lot from his logical thinking, rigorous attitude and constructive advice during the last two years. It has been my great honor to be part of his research team and all the works I have achieved in this thesis couldn't have been done without him.

I would also like to thank my thesis committee members and examiners, Dr. Han-Ping Hong, Dr. Craig Miller and Dr. Takashi Kuboki, for their valuable time and efforts in giving sound suggestions to my thesis. All their opinions contributed to the quality of my thesis are greatly appreciated.

The financial support from TransCanada Pipelines Limited, Natural Sciences and Engineering Research Council of Canada (NSERC), the University of Western Ontario and Dr. Wenxing Zhou was essential to the accomplishment of the study in this thesis and is greatly acknowledged.

The help and companion from my colleagues in our research group and all my friends in Canada are much appreciated, my life in the past two years wouldn't be so happy and colorful otherwise.

Lastly, all my gratitude and appreciation would go to my family for their continual support and endless love.

Table of Contents

List of Tables

List of Figures

Chapter 1 Introduction

1.1 Background

Transmission pipelines are the safest and most effective way to transport a large volume of natural gas over a long distance. There are approximately 78,000 and 480,000 km gas transmission pipelines in Canada and the United States, respectively. Although rare, pipeline incidents do occur due to various causes such as the third-party excavation activities, corrosion, material failure, ground movement and incorrect operation. In many jurisdictions around the world, pipeline operators are required to report pipeline incidents to regulatory agencies (Golub et al. 1996; Kiefner et al. 2001; EGIG 2014). These historical pipeline failure incidents provide valuable information about the leading causes for pipeline failures, typical failure modes, failure rate in terms of per year per unit length, consequences of failures, etc. Such information will facilitate the development of effective pipeline integrity management programs and provide baseline statistics for the quantitative risk assessment of pipelines. Since 1970, the Pipeline and Hazardous Material Safety Administration (PHMSA) of the United States Department of Transportation (DOT) has collected detailed information about incidents that occurred on oil and gas pipelines regulated by PHMSA and met certain incident reporting criteria. The PHMSA pipeline incident data are accessible to the general public at http://www.phmsa.dot.gov/pipeline/library/data-stats. The PHMSA incident data for gas transmission pipelines between 1970 and 1993 were analyzed by Golub et al. (1996). Kiefner et al. (2001) analyzed the PHMSA incident data for gas transmission and gathering pipelines between 1985 and 1997. However, analyses of the more recent PHMSA incident data have not been reported in the literature. An ignited full-bore rupture of a natural gas transmission pipeline can have enormously severe consequences in terms of the human safety and property damage (Nessim et al. 2009; Zhou and Nessim 2011). To quantitatively evaluate the risk associated with a given gas pipeline, it is therefore critically important to evaluate the probability of ignition (POI) of the pipeline given rupture. The ignition/non-ignition information included in the historical pipeline

failure incident data provides an opportunity to identify key pipeline attributes that impact POI and subsequently develop an appropriate POI model.

1.2 Objective and Scope

The study reported in this thesis is part of a Collaborative Research and Development (CRD) program funded by the Natural Sciences and Engineering Research Council (NSERC) of Canada and TransCanada Pipelines Limited. The objectives of this study are to 1) carry out statistical analyses of the PHMSA onshore gas transmission pipeline incident data to gain insights into the current state of onshore gas transmission pipelines in the US and develop relevant failure rate statistics that can be employed as the baseline failure probabilities for carrying out system-wide risk assessments of pipelines; 2) propose a POI model for ruptures of onshore gas transmission pipelines based on the corresponding PHMSA incident data to facilitate the quantitative risk assessment of gas pipelines, and 3) illustrate the application of outcomes of tasks 1) and 2) through the quantitative risk assessment of a hypothetical gas pipeline example.

The three main topics of this study are presented in Chapters 2, 3, and 4, respectively. Chapter 2 presents the statistical analyses of the mileage and pipe-related incident data for onshore gas transmission pipelines based on the PHMSA database between 2002 and 2013. The PHMSA data were analyzed to obtain the breakdowns of the overall pipeline mileage and incidents by different pipeline attributes. Chapter 3 presents the development of the POI model for ruptures of onshore gas transmission pipelines. The log-logistic POI model is developed based on the PHMSA incident data between 2002 and 2014 using the maximum likelihood method. In Chapter 4, quantitative risk assessments of a hypothetical onshore gas transmission pipeline is carried out to evaluate the societal and individual risk levels associated with ruptures of the pipeline, based on the failure statistics and POI model obtained in Chapters 2 and 3, respectively.

1.3 Thesis Format

This thesis is prepared in an Integrated-Article Format as specified by the School of Graduate and Postdoctoral Studies at the University of Western Ontario, London ON,

Canada. A total of five chapters are included in the thesis. Chapter 1 gives a brief introduction of the background, objective and scope of the study. The main body of the thesis includes Chapters 2, 3, and 4, each of which is presented in an integrated-article format without an abstract, but with its own references. Chapter 5 presents the summary and conclusions of this thesis, and recommendations for future study.

References

EGIG 2014. Gas pipeline incidents: 9th report of the European Gas Pipeline Incident Data Group (period 1970 – 2013). EGIG 14.R.0403, European Gas Pipeline Incident Data Group, NL – 9700 Ma Groningen.

Golub, E., Greenfeld, J., Dresnack, R., Griffis, F.H. and Pignataro, L.J. 1996. Pipeline accident effects for natural gas transmission pipelines. DTRS 56-94-C-0006, National Technical Information Service, Springfield, Virginia 22161.

Kiefner, J.F., Mesloh, R.E. and Kiefner, B.A. 2001. Analysis of DOT reportable incidents for gas transmission and gathering system pipelines, 1985 through 1997. L51830e, Technical Toolboxes, Inc., Houston, Texas 77098.

Nessim, M.A., Zhou, W., Zhou, J. and Rothwell, B. (2009). Target reliability levels for design and assessment of onshore natural gas pipelines. Journal of Pressure Vessel Technology, ASME, 131(12), 061701, 1-12.

Zhou, W., and Nessim, M.A. 2011. Optimal design of onshore natural gas pipelines. Journal of Pressure Vessel Technology, 133(3): 031702.

Chapter 2

Statistical Analyses of Incidents on Onshore Gas Transmission Pipelines Based on PHMSA Database

2.1 Introduction

Since 1970, the Pipeline and Hazardous Material Safety Administration (PHMSA) within the United States Department of Transportation (DOT) has collected information on incidents that occurred on gas and liquid pipelines regulated by PHMSA and met established reporting criteria. It is noted that incident is synonymous with failure in the context of this study. PHMSA's pipeline incident report includes information such as the location, cause and consequences of the incident as well as the basic attributes (e.g. diameter, wall thickness, steel grade, operating pressure etc.) of the pipeline involved in the incident. The incident data can be accessed from http://www.phmsa.dot.gov/pipeline/library/data-stats. In addition to the incident data, PHMSA also collects annual reports from gas and liquid pipeline operators that contain general information such as the total pipeline mileage, transported commodities, mileage by material and installation dates. The pipeline incident and mileage data provide valuable information for researchers and industry professionals to identify major threats to the structural integrity of oil and gas pipelines, carry out system-wide risk assessments and develop effective risk mitigation strategies. The study reported in this chapter was focused on the PHMSA incident and mileage data associated with the onshore (as opposed to offshore) gas transmission (as opposed to gathering) pipelines, which account for the vast majority of gas pipelines in the US.

Golub et al. (1996) analyzed the PHMSA incident data on the gas transmission pipelines between 1970 and 1993. They found that the primary causes of incidents were the outside force, construction-material defect and corrosion, responsible for 40.89, 27.65 and 17.90% of all incidents, respectively. Only incident rates due to corrosion were estimated, which are 0.14, 0.59, 0.17 and 0.40 per 1000 miles per year (i.e. 8.70×10^{-5}, 3.67×10^{-4}, 1.06×10^{-4} and 2.49×10^{-4} per km per year) for coated, uncoated, cathodically

protected and unprotected pipes, respectively. They identified that outside force incidents were primarily due to inadequate depth of cover and that larger pipe wall thickness led to better pipeline safety and reduced incident rates. It was observed that the electric resistance welded pipes installed in the 1940s and 1970s had high rates of material failure.

Kiefner et al. (2001) analyzed the incidents on the gas transmission and gathering pipelines from 1985 to 1997 as reported in the PHMSA database. The primary causes for incidents were identified as the third-party damage, internal corrosion and external corrosion, responsible for 28.4%, 12.0% and 10.1% of all incidents, respectively. The authors also examined the variation of the number of incidents due to different failure causes with time. For example, the number of incidents due to the third-party damage generally decreased with time, which was partly attributed to the increasing use of the one-call system. The number of leaks was found to decrease with time, probably due to the growing use of the in-line inspection. Kiefner et al. further evaluated the incident rates (per mile per year) due to the third-party damage and external corrosion using the incident and mileage data. For example, the incident rate due to the third-party damage for pipelines with outside diameters less than 4 inches was evaluated to be 1.01×10^{-4} per mile per year (i.e. 6.28×10^{-5} per km per year), and the incident rate due to external corrosion for coated cathodically protected pipelines was calculated to be 1.56×10^{-5} per mile per year (i.e. 9.69×10^{-6} per km per year).

More pipeline incident and mileage data have been added to the PHMSA database since the completion of the aforementioned studies, which are close to two decade old. Therefore, it is desirable to carry out analyses of the up-to-date PHMSA database to gain insights into the current state of gas transmission pipelines in the US and develop relevant failure statistics that can serve as the baseline failure probabilities for carrying out system-wide risk assessments of pipelines. This is the objective of the study reported in this chapter.

The PHMSA database is updated on an annual basis. At the time of this study, the PHMSA database for the onshore gas transmission pipelines includes the incident data, from 1970 to 2014, and the mileage data from 1970 to 2013. The present study analyzed the incident and mileage data from 2002 to 2013. The 2014 incident data were excluded because the corresponding mileage data were unavailable; therefore, it was not feasible to evaluate the incident rates for 2014. The pre-2002 data were excluded from the study because the information included in the data is much less detailed than that included in the post-2002 incident data as discussed in Section 2.3.2, which makes it very difficult to combine the data in these two periods together for analysis. Furthermore, the breakdown of the post-2002 pipeline mileage data by the pipeline attributes (e.g. diameter, year of installation, location class, etc.) is more detailed than that of the pre-2002 mileage data, allowing more refined evaluations of incident rates by pipeline attributes. Finally, the incident and mileage data between 2002 and 2013 are considered reasonably representative of the current state of onshore gas transmission pipelines in the US.

The rest of this chapter is organized as follows. Section 2.2 presents the pipeline mileage data to provide an overview of the onshore gas transmission pipeline networks in the US and put the incident data described in Section 2.3 into perspective. The rupture rate analyses using both the incident and mileage data are included in Section 2.4. Section 2.5 summarizes the main findings of the study.

2.2 PHMSA Pipeline Mileage Data

The mileage data of gas transmission and distribution pipelines are submitted in annual reports to PHMSA by pipeline operators, following the requirements in Part 191 of Title 49 of the Code of Federal Regulations (CFR) (USOFR 2013). The total lengths of the onshore natural gas transmission pipelines in the US from 2002 to 2013 are shown in Fig. 2.1. The figure shows that there was little change in the total length between 2002 and 2013. The total length varied between 470,103 and 481,148 km within the 12-year period, with the 12-year average length of 477,149 km. Since 2009, the total length has remained almost unchanged at around 480,000 km.

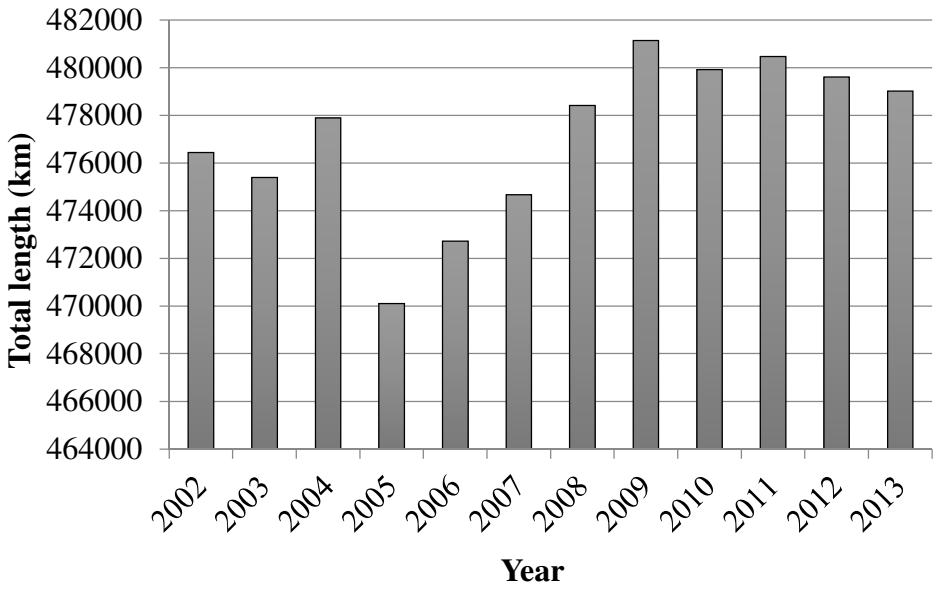

Figure 2.1 Total lengths of onshore gas transmission pipelines between 2002 and 2013

Figure 2.2 shows the breakdown of the total length by the pipe (outside) diameter (d, inches), where "Unk." denotes unknown. The figure indicates that the change in the breakdown with time is small and that 40-50% of the pipelines have diameters between 10 and 28 inches. The percentage of pipelines with $d > 28$ inches appears to gradually increase over time. The breakdown of the total length by the year of installation is shown in Fig. 2.3, which shows that older pipelines are gradually replaced by newer pipelines between 2002 and 2013. However, there were still approximately 60% of the pipelines more than 45 years old as of 2013.

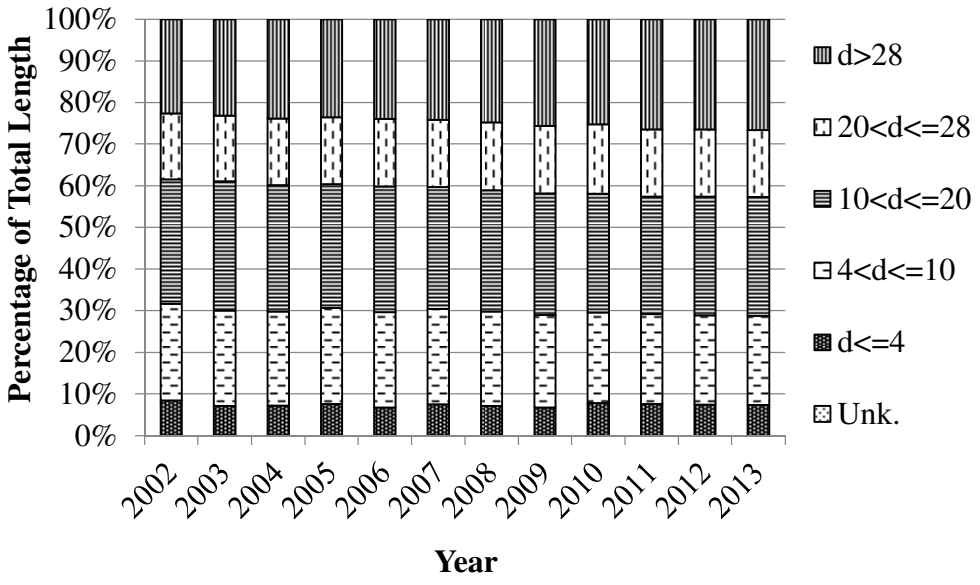

Figure 2.2 Distribution of total mileage by diameter from 2002 to 2013

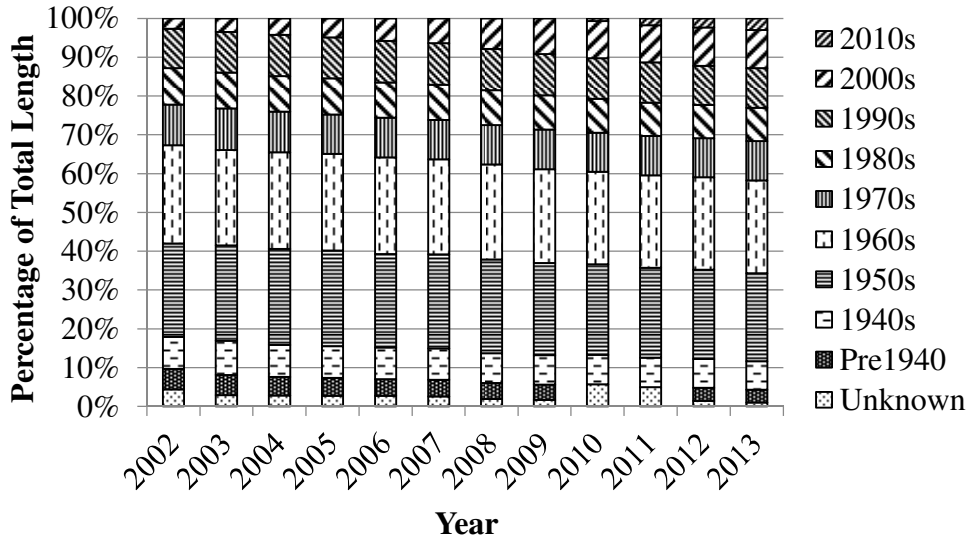

Figure 2.3 Distribution of total mileage by year of installation from 2002 to 2013

A key consideration in the design of a natural gas transmission pipeline is the location class of the pipeline. The location class is a geographic area along the pipeline classified primarily according to the number and proximity of buildings intended for human occupancy (USOFR 2013); in other words, the location class characterizes the population

density along the pipeline. According to ASME B31.8 (ASME 2013) and Part 191, Title 49 of CFR (USOFR 2013), there are four location classes for gas pipelines, namely Class 1, Class 2, Class 3 and Class 4. The Class 1 represents sparsely populated areas such as wasteland, deserts and farmland; the Class 2 reflects fringe areas around cities and towns, industrial areas, ranch or country estates, etc.; the Class 3 reflects areas such as suburban housing developments, shopping centers, residential areas, etc., and the Class 4 represents city centers where multistory buildings (defined as having four or more floors above ground) are prevalent and traffic is heavy (ASME 2013).

According to ASME B31.8, the wall thickness, wt_n, of a steel gas transmission pipeline in the US is in general determined as follows:

$$wt_n = \frac{P \cdot d}{2 \cdot F \cdot SMYS} \tag{2.1}$$

where P is the design pressure; F is a safety factor that depends on the location class, and SMYS is the specified minimum yield strength. Note that F decreases as the location class of the pipeline increases. Given the diameter, design pressure and SMYS, the wall thickness of a higher location class pipeline is therefore greater than that of a lower location class pipeline to afford more protections for the pipeline as well as its surrounding population. The breakdown of the total length by the location class is shown in Fig. 2.4. The figure indicates that the vast majority of the pipelines (about 80%) are in Class 1 areas, whereas about 10% of the pipelines are in Class 2 and Class 3 areas, respectively, with very few pipelines in Class 4 areas.

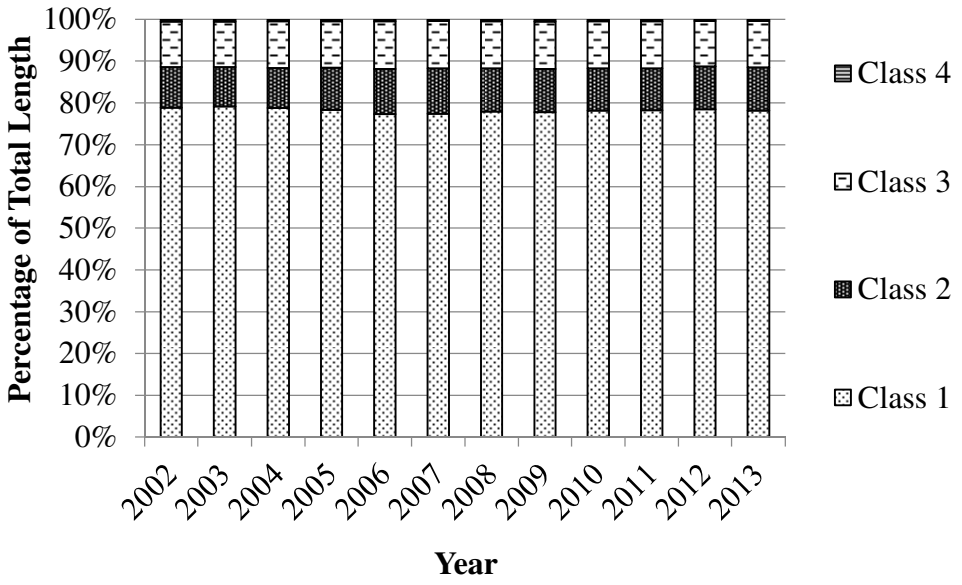

Figure 2.4 Distribution of total mileage by location class between 2002 and 2013

Analyses of the mileage data indicate that steel is the predominant pipe material: steel pipelines consistently account for over 99% of the total pipeline length between 2002 and 2013. The rest of the pipelines are made of materials such as cast iron, wrought iron and plastic. Corrosion prevention measures are often employed on steel pipelines. Commonly used measures include either coating or cathodic protection or both. The breakdown of the length of steel pipelines by the corrosion prevention measure is shown in Fig. 2.5, where CB, CC, NB and NC denote cathodically protected bare, cathodically protected coated, non-cathodically protected bare and non-cathodically protected coated steel pipelines, respectively. Note that the breakdown of the mileage data by the corrosion prevention measure for years 2010 and 2011 is unavailable in the PHMSA database. Figure 2.5 shows that about 97-98% and 1-2% of the steel pipelines are CC and CB pipelines, respectively, whereas the lengths of NC and NB steel pipelines are negligible.

One observation of the PHMSA pipeline mileage data is that the data structure does not permit breakdown of the mileage by more than one pipeline attribute. For example, it is not feasible to know the length of Class 1 pipelines with diameters between 10 and 20

inches, or the length of Class 2 pipelines installed in the 1980s. As a result of this limitation, which was also pointed out by Kiefner et al. (2001), it is not feasible to evaluate the incident rates considering more than one pipeline attribute. Therefore, it is suggested that the PHMSA reporting format of the pipeline mileage data be revised in the future to allow more detailed breakdown of the mileage and facilitate more detailed evaluation of the incident rate.

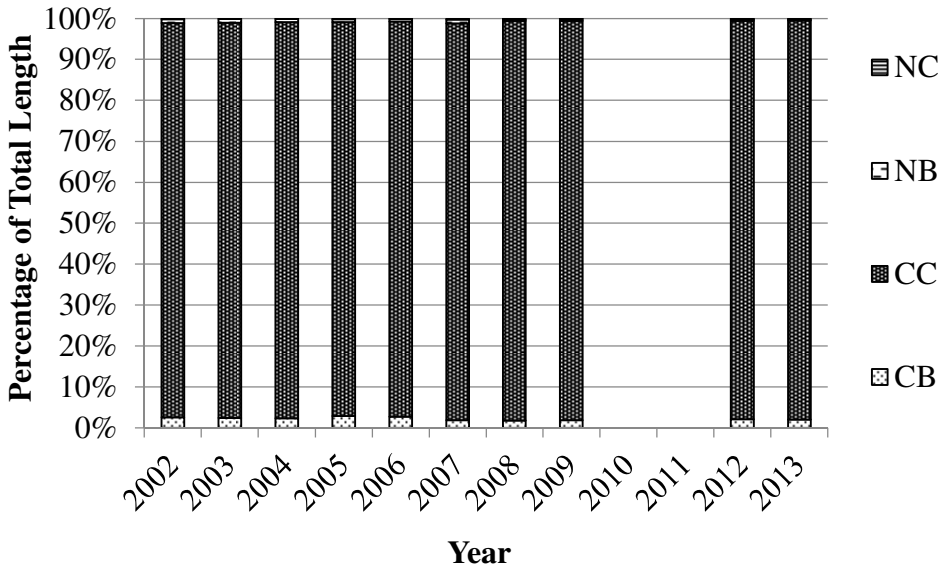

Figure 2.5 Breakdown of the length of steel pipelines by corrosion prevention measure between 2002 and 2013

2.3 PHMSA Pipeline Incident Data

2.3.1 Reporting Criteria and Brief History

Title 49 of the Code of Federal Regulations Parts 191, 195 (USOFR 2013) requires that the pipeline operator submit an incident report within 30 days of a pipeline incident or accident, if the incident or accident meets the reporting criteria. According to the current regulation, an incident or accident on a gas pipeline is reportable if any of the following three criteria is met.

(1) An event that involves a release of gas from a pipeline, or of liquefied natural gas (LNG), liquefied petroleum gas, refrigerant gas, or gas from an LNG facility and that results in one or more of the following consequences:

(i) A death, or personal injury necessitating in-patient hospitalization;

(ii) Estimated property damage of $50,000 or more, including loss to the operator and others, or both, but excluding cost of gas lost;

(iii) Unintentional estimated gas loss of three million cubic feet or more;

(2) An event that results in an emergency shutdown of an LNG facility.

(3) An event that is significant in the judgment of the operator, even though it does not meet (1) or (2) above.

It follows from the above that the PHMSA database does not include *all* pipeline incidents but rather includes incidents that are considered significant according to the criteria established in CFR. Note that the reporting threshold of $50,000 for property damage has not been changed or adjusted for inflation since 1984. Therefore, inflation may cause more incidents to become reportable in later years of the period from 1985 to present.

The incident reports submitted by pipeline operators are based on a standard form (Form 71002) provided by DOT. Since 1970, the format of the standard form underwent three significant changes in 1984, 2002 and 2010, respectively; therefore, the PHMSA incident data have four different formats. The number of data fields in the PHMSA incident database decreased from 149 to 81 after the 1984 change, increased from 81 to 195 after the 2002 change, and further increased from 195 to 552 after the 2010 change. In general, the information about a given incident collected by PHMSA has become more detailed and elaborate over time. In addition to significantly more data fields having been added to the database since 2002, the descriptions of some of the fields have been changed over

time, which gives rise to difficulties in combining the incident data from all periods into a single set of data for analyses.

The incidents in the PHMSA database are classified as either pipe-related or non-pipe related. Pipe-related incidents include those occurring on body of pipe and pipe seam, whereas non-pipe related incidents include those occurring on compressors, valves, meters, hot tap equipment, filters and so on. Only pipe-related incidents were analyzed in this study.

2.3.2 Data Aggregation

The present study focused on analyzing the PHMSA incident data within the period of 2002 to 2013. As indicated in Section 2.3.1, the format of the incident data before 2010 is different from that after 2010; therefore, care needs to be taken to aggregate the data from the two periods together. The two main considerations in the data aggregation are the cause of the incident (i.e. failure cause) and mode of the pipeline failure due to the incident. Between 2002 and 2009, there were seven main failure causes, namely corrosion, natural forces, excavation, other outside forces, material and welds, equipment and operations, and other. Each main failure cause consists of certain number of secondary causes; for example, corrosion consists of internal and external corrosions. After 2010, eight main failure causes were included: corrosion, natural forces, excavation, other outside forces, material failure of pipe or weld, equipment failure, incorrect operation and other. Each main failure is further divided into several secondary failure causes. The main and secondary failure causes for the periods of 2002-2009 and after 2010 are summarized in Table 2.1.

For the purpose of the data aggregation, the sets of failure causes identified in the periods of 2002-2009 and 2010-2013 were mapped to a single set of failure causes adopted in this study. The mapping is shown in Table 2.1. Note that the set of failure causes adopted in this study are to a large extent consistent with those identified after 2010. Note also that although the failure cause "Other" employed in this study is corresponding to a significant number of secondary failure causes in both 2002-2009 and 2010-2013, the

contribution of each individual cause to the overall number of incidents is relatively small. For example, the failure causes “incorrect operation”, “equipment failure” and “heavy rains/floods” only account for 1.1%, 1.5% and 0.9%, respectively, of the overall number of pipe-related incidents; therefore, it is considered reasonable to combine them into one main failure cause category.

Table 2.1 Mapping of failure causes for the two report formats

2002-2009		2010-2013		Failure causes adopted in this study (acronym)
Corrosion	Internal corrosion	Corrosion	Internal corrosion	Internal corrosion (IC)
	External corrosion		External corrosion	External corrosion (EC)
Material and welds	Body of pipe	Material failure of pipe or weld		Material failure (MF)
	Component			
	Joint			
	Butt			
	Fillet			
	Pipe seam			
			Construction-, installation-, or fabrication-related	
			Original manufacturing-related(not girth weld or other welds formed in the field)	
			Environmental cracking-related	
Excavation	Third party excavation damage	Excavation	Excavation damage by third party	Third-party excavation (TPE)
	Operator excavation damage (includes contractors)		Excavation damage by operator (first party)	First- and second-party excavation (FSPE)
			Excavation damage by operator's contractor (second party)	
Other outside forces	Rupture of previously damaged pipe		Previous damage due to excavation activity	Previously damaged pipe (PDP)
		Other outside forces	Previous mechanical damage not related to excavation	
	Car, truck or other vehicle not related to excavation activity		Damage by car, truck, or other motorized vehicle/equipment not engaged in excavation	Vehicle not engaged in excavation (V)
	Fire/explosion as primary cause of failure		Nearby industrial, man-made, or other fire/explosion as primary cause of incident	Other (O)
	Vandalism		Intentional damage	
			Damage by boats, barges, drilling rigs, or other maritime equipment or vessels set adrift or which have otherwise lost their mooring	
			Routine or normal fishing or other maritime activity not engaged in excavation	
			Electrical arcing from other equipment or facility	
			Other outside force damage	

Equipment and operations	Malfunction of control/relief equipment	Equipment failure	Malfunction of control/relief equipment	
	Threads stripped, broken pipe coupling		Threaded connection/coupling failure	
	Ruptured or leaking seal/pump packing			
			Compressor or compressor-related equipment	
			Non-threaded connection failure	
			Defective or loose tubing or fitting	
			Failure of equipment body(except compressor), vessel plate, or other material	
			Other equipment failure	
	Incorrect operation	Incorrect operation	Damage by operator or operator's contractor not related to excavation and not due to motorized vehicle/equipment damage	
			Underground gas storage, pressure vessel, or cavern allowed or caused to overpressure	
			Valve left or placed in wrong position, but not resulting in an overpressure	
			Pipeline or equipment overpressured	
			Equipment not installed properly	
			Wrong equipment specified or installed	
			Other incorrect operation	
Other	Miscellaneous	Other	Miscellaneous	
	Unknown		Unknown	
Natural forces	Heavy rains/floods	Natural forces	Heavy rains/floods	
	Temperature		Temperature	
	High winds		High winds	
	Lightning		Lightning	
			Other natural force damage	
	Earth movement		Earth movement	Earth movement (EM)

Another consideration in the data aggregation is the failure mode of the pipeline in a given incident. Three failure modes were identified for the incident data between 2002 and 2009 (see Table 2.2): leak, rupture and other. A leak is further categorized as a pinhole, connection failure or puncture, whereas a rupture is further classified as a circumferential or longitudinal rupture. The incident data for the period of 2010-2013 included four failure modes (see Table 2.2): mechanical puncture, leak, rupture and other.

A leak is further classified as a pinhole, crack, connection failure, seal or packing or other type of leak, whereas a rupture is classified as a circumferential, longitudinal or other type of rupture. Similar to the mapping of the failure causes, the two sets of failure modes identified in the two reporting periods were mapped to a single set of failure modes in this study, as shown in Table 2.2.

Table 2.2 Mapping of failure modes for the two report formats

<table>
<tr><th colspan="2">2002-2009</th><th colspan="2">2010-2013</th><th>Failure modes adopted in this study</th></tr>
<tr><td rowspan="6">Leak</td><td>Pinhole</td><td rowspan="5">Leak</td><td>Pinhole</td><td rowspan="5">Leak</td></tr>
<tr><td></td><td>Crack</td></tr>
<tr><td>Connection failure</td><td>Connection failure</td></tr>
<tr><td></td><td>Seal or packing</td></tr>
<tr><td></td><td>Other leak type</td></tr>
<tr><td>Puncture</td><td colspan="2">Mechanical puncture</td><td>Puncture</td></tr>
<tr><td rowspan="3">Rupture</td><td>Circumferential</td><td rowspan="3">Rupture</td><td>Circumferential</td><td rowspan="3">Rupture</td></tr>
<tr><td>Longitudinal</td><td>Longitudinal</td></tr>
<tr><td></td><td>Other of rupture type</td></tr>
<tr><td colspan="2">Other</td><td colspan="2">Other</td><td>Other</td></tr>
</table>

2.3.3 Incident Data Analysis

2.3.3.1 Distribution of incidents by failure cause

Between 2002 and 2013, a total of 464 pipe-related incidents on onshore gas transmission pipelines were reported to PHMSA. The distribution of these incidents with respect to the set of failure causes adopted in this study is shown in Fig. 2.6. The figure shows that the third-party excavation (TPE), external corrosion (EC), material failure (MF) and internal corrosion (IC), in the order of descending contributions, are the four most common failure causes and responsible for over 75% of the 464 incidents. In particular, TPE and EC are responsible for half of all incidents, with the contribution of TPE slightly higher than that of EC. Note that EC and IC are responsible for about 32% of all incidents, markedly larger than the proportion of incidents due to corrosion (17.9%) among all incidents on US gas transmission pipelines obtained by Golub et al. in 1996 and that among all incidents on US gas transmission and gathering pipelines (22.1%) obtained by Kiefner et al. in 2001. The breakdowns of all incidents and of those

incidents due to TPE, EC, MF and IC by various pipeline attributes, the failure mode and failure consequences are presented in the following sections.

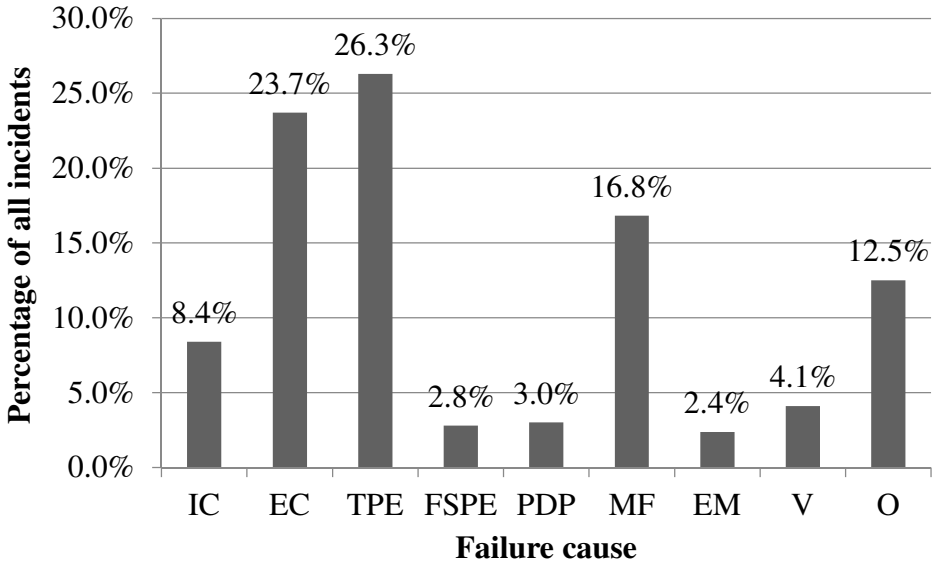

Figure 2.6 Distribution of all pipe-related incidents between 2002 and 2013 by failure cause

2.3.3.2 Distributions of incidents by pipeline attributes

The breakdowns of the number of incidents by four pipeline attributes, namely the diameter, year of installation, location class and corrosion prevention measures are presented in this section. The distribution of the total number of incidents by the diameter is shown in Fig. 2.7. The figure shows that about 76% of the incidents occurred on pipelines with $4 < d \leq 28$ inches. The proportions of incidents on pipelines with $d < 4$ inches and $4 < d \leq 10$ inches are remarkably consistent with the proportions of the corresponding lengths in the overall pipeline mileage (see Fig. 2.2). On the other hand, the proportions of incidents on pipelines with $10 < d \leq 20$ inches, and $d > 20$ inches are somewhat higher and lower, respectively, than the proportions of the corresponding lengths.

The breakdowns of the TPE-, EC-, MF- and IC-caused incidents by diameter are shown in Fig. 2.8. It is interesting to note that the majority of the incidents due to TPE (79.5%) or IC (84.6%) occurred on pipelines with small or medium diameters (i.e. $4 < d \leq 20$ inches). On the other hand, the majority of the incidents due to EC (79.1%) or MF (87.2%) occurred on pipelines with medium or large diameters (i.e. $d > 10$ inches). The concentration of TPE-caused incidents on pipelines with small or medium diameters can be explained by the fact that such pipelines tend to have relatively small wall thicknesses and therefore are more likely to fail once impacted in the excavation. It is however unclear as to the reason that EC-caused incidents occurred more frequently on pipelines with relatively large diameters than IC-caused incidents.

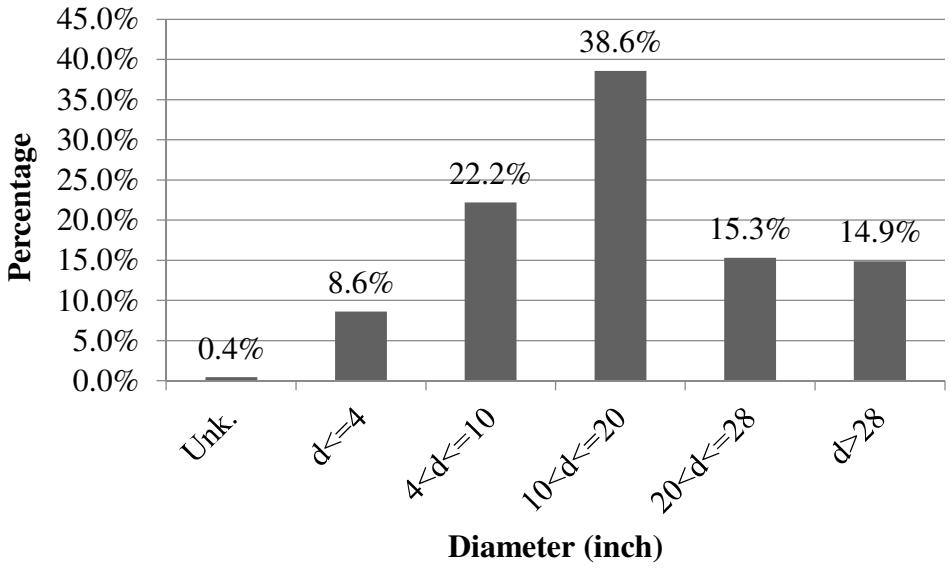

Figure 2.7 Distribution of all incidents by diameter

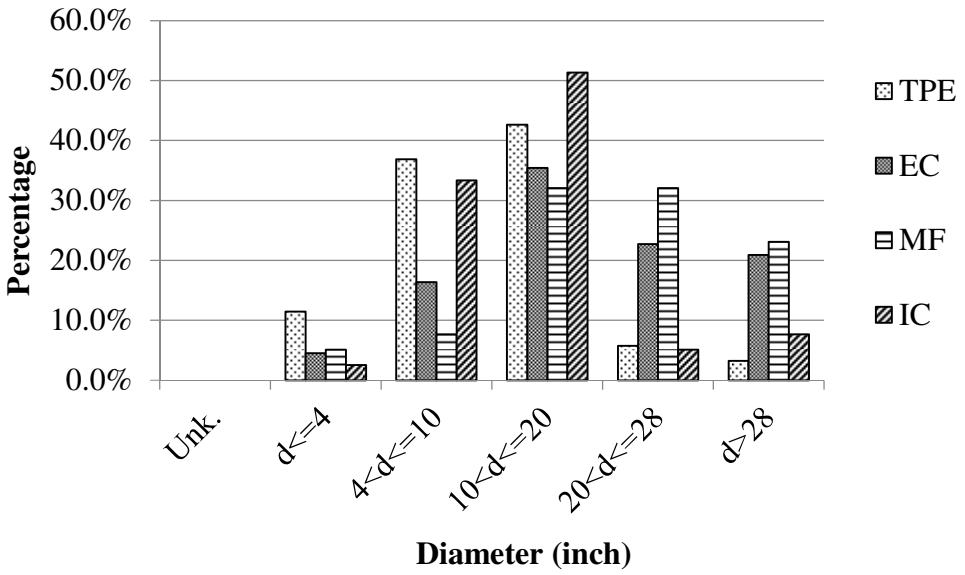

Figure 2.8 Distribution of incidents due to TPE, EC, MF and IC by diameter

The distribution of the incidents by the year of installation of the pipeline is depicted in Fig. 2.9. The figure shows that 53% of the incidents occurred on pipelines installed in the 1950s and 1960s. This is generally consistent with the proportion of the length of such pipelines in the overall mileage as shown in Fig. 2.3. The figure also suggests, not surprisingly, that in general incidents are more likely to occur on older pipelines than on newer pipelines. The breakdown of the numbers of incidents due to TPE, EC, MF and IC by the year of installation is shown in Fig. 2.10. Fifty percent of the MF-caused incidents occurred on pipelines installed in the 1950s. Given that the pipelines installed in the 1950s account for only about 20% of the total mileage (see Fig. 2.3), it can be inferred that the pipes or field-welding or both in that period are of relatively poor quality. The breakdowns of EC- and IC-caused incidents by the year of installation are in general similar. However, it is noteworthy that a significant portion (about 20%) of IC-caused incidents occurred on pipelines installed in the 1980s.

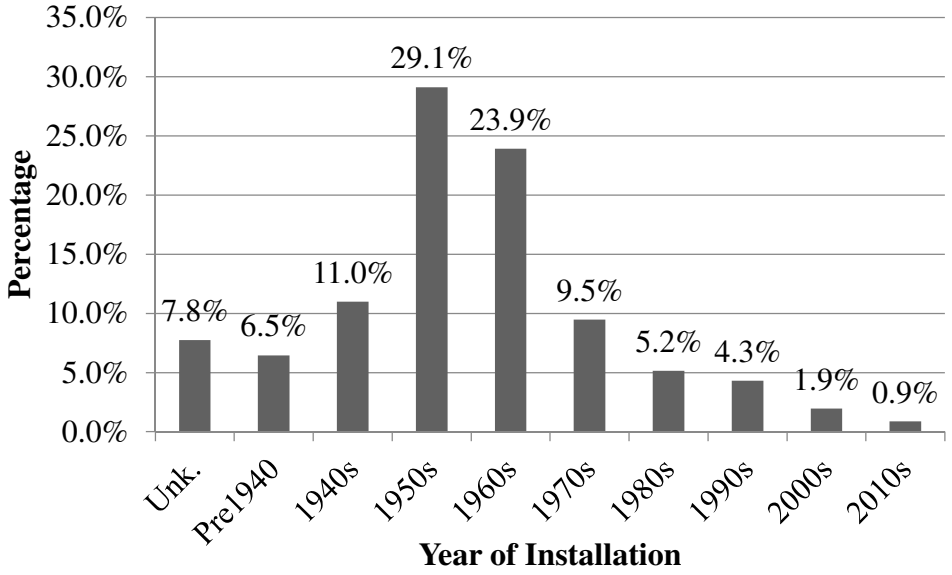

Figure 2.9 Distribution of all incidents by year of installation

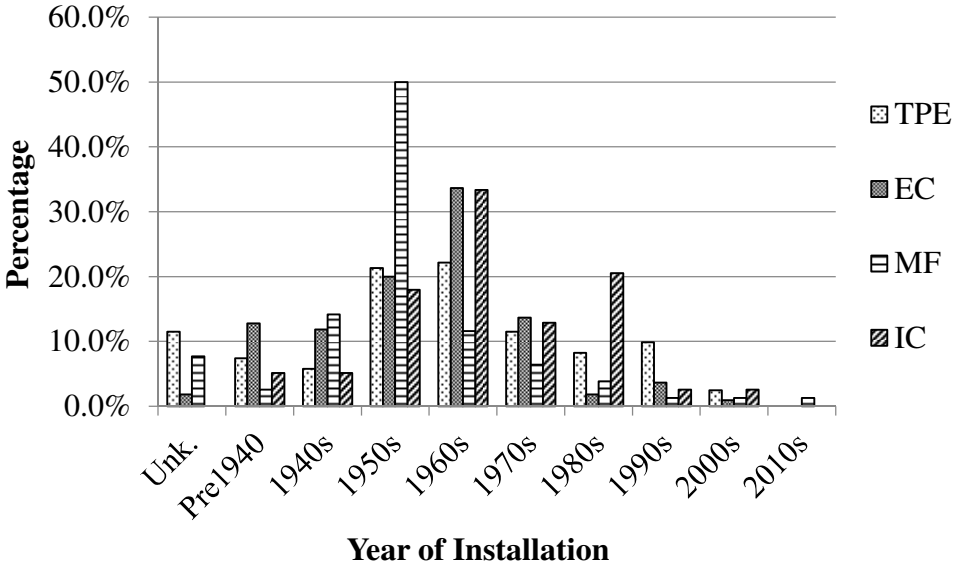

Figure 2.10 Distribution of incidents due to TPE, EC, MF and IC by year of installation

The distribution of the incidents by the location class is depicted in Fig. 2.11. The distribution is consistent with the proportions of the lengths of pipelines in the four

location classes as shown in Fig. 2.4. The distributions of the incidents due to TPE, EC, MF and IC by the location class are shown in Fig. 2.12. Two observations can be made from the figure. First, the vast majority (95%) of the IC-caused incidents occurred on Class 1 pipelines, which is markedly more than the proportion (about 80%) of the length of Class 1 pipelines. Second, a significant portion (20%) of the TPE-caused incidents occurred on Class 3 pipelines. This can be explained by the fact that the relatively high population density associated with Class 3 generally results in more excavation activities and a higher likelihood of the pipelines being impacted.

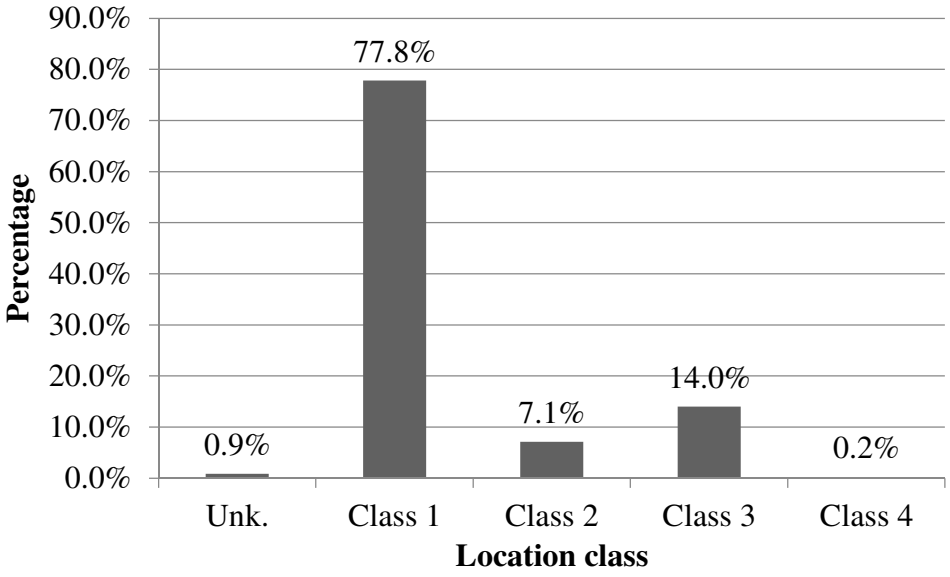

Figure 2.11 Distribution of all incidents by location class

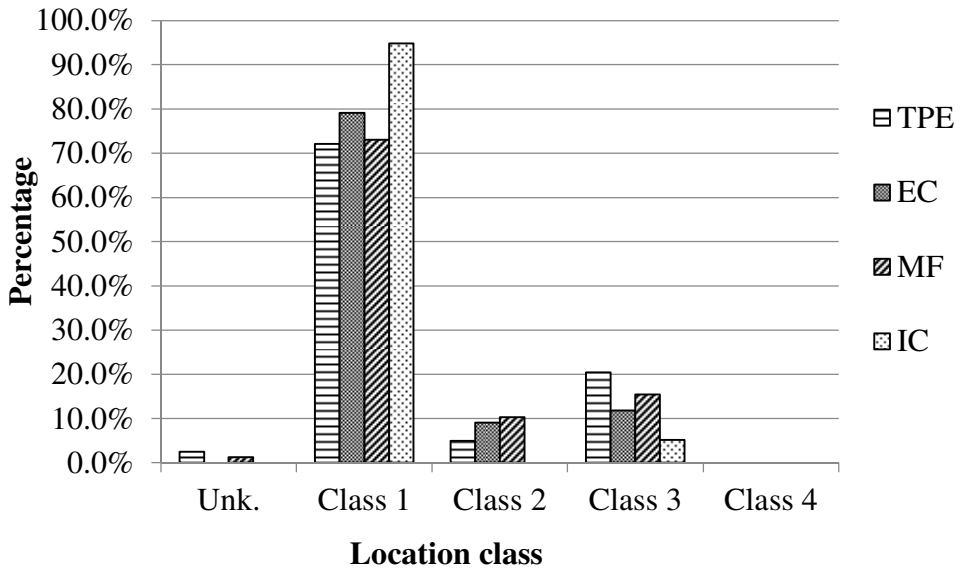

Figure 2.12 Distribution of incidents due to TPE, EC, MF and IC by location class

It was observed that 99.4% of the incidents occurred on steel pipelines, which is consistent with the proportion of the length of steel pipelines as described in Section 2.2. The distributions of EC- and IC-caused incidents on steel pipelines by the corrosion prevention measure are shown in Fig. 2.13. The figure shows that 81% of EC-caused incidents and 88% of IC-caused incidents occurred on CC steel pipelines, both percentages markedly lower than the proportion (about 97-98%) of the length of CC pipelines. On the other hand, 19% of EC-caused incidents and 12% of IC-caused incidents occurred on CB/UB/UC pipelines, both percentages markedly higher than the proportion (less than 3%) of the length of such pipelines. This demonstrates the effectiveness of cathodical protection and coating in preventing corrosion on steel pipelines.

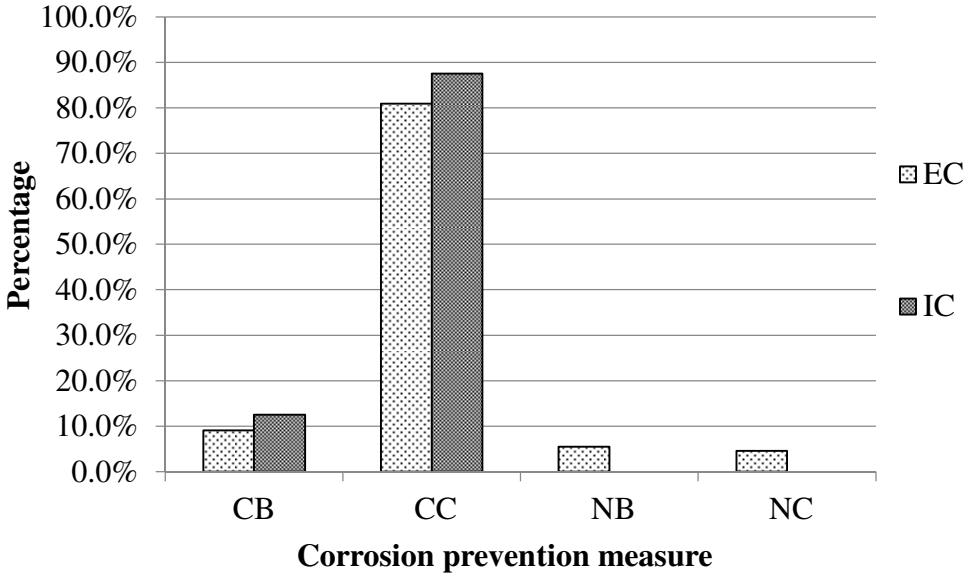

Figure 2.13 Distribution of incidents due to EC and IC by corrosion prevention measure

2.3.3.3 Distributions of incidents by failure mode and ignition

The distribution of the incidents by the set of failure modes adopted in this study (see Table 2.2) is shown in Fig. 2.14. The figure indicates that rupture is the most common failure mode with 38% of the incidents resulting in ruptures, followed by leak (30%) and puncture (20%). Given that different failure modes can have drastically different failure consequences (e.g. the impact zone associated with an ignited rupture can be much larger than that of an ignited leak), the breakdowns of the incidents by all failure modes and failure causes were analyzed and are shown in Fig. 2.15. The figure indicates that a little over 50% of EC- and IC-caused incidents resulted in ruptures. The majority of the TPE-caused incidents resulted in punctures (about 60%), followed by ruptures (22%). Very few leaks resulted from TPE-caused incidents. The percentages of leaks and ruptures resulting from MF-caused incidents are approximately 55 and 35%, respectively. Finally, the majority (between 70-80%) of the incidents due to previously damaged pipe (PDP) and earth movement (EM) resulted in ruptures.

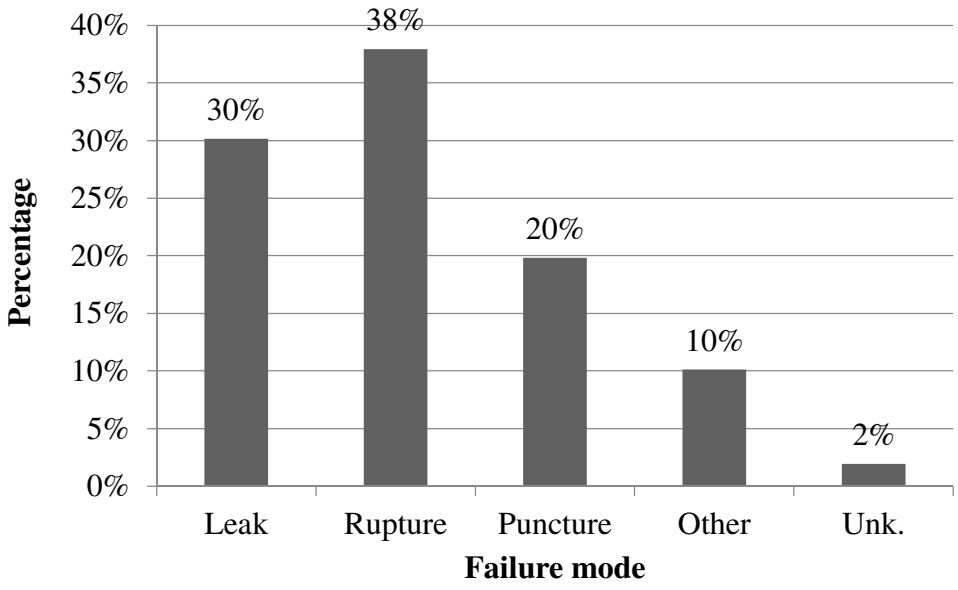

Figure 2.14 Distribution of incidents by failure mode

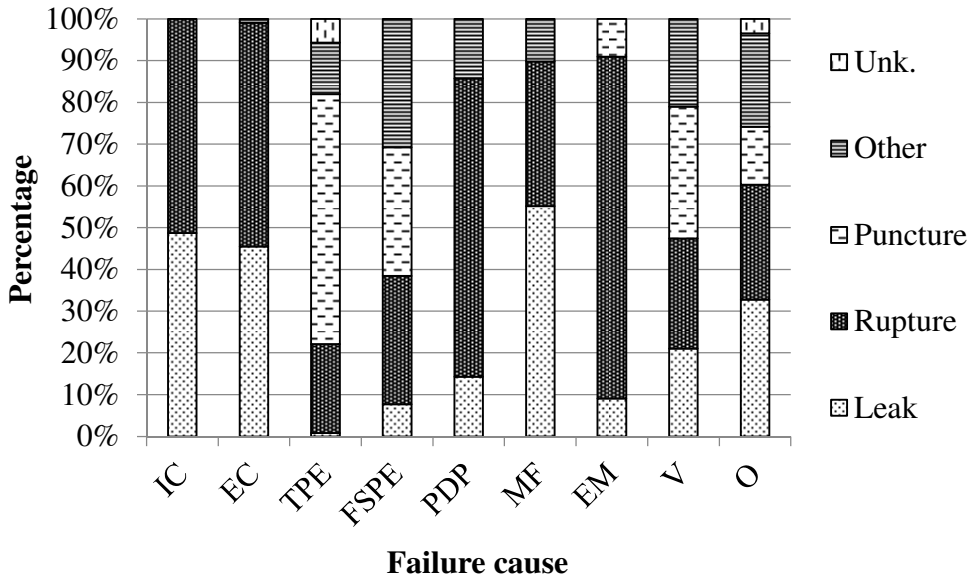

Figure 2.15 Distribution of incidents by failure mode for each failure cause

The consequences of ignited incidents of gas transmission pipelines are far more severe than those of non-ignited incidents. Therefore, it is valuable to examine the distribution of the incidents by ignition. This is shown in Fig. 2.16. The figure indicates that the

majority (85%) of the incidents did not involve ignition. For those ignited incidents, about half of them also lead to explosions. Note that ignition means only a jet fire is created in the incident whereas explosion means that a fireball precedes the jet fire. The distributions of the incidents by ignition and the failure cause are show in Fig. 2.17. It is worth pointing out that all ignited incidents caused by earth movement lead to explosions, whereas no incidents caused by vehicles not engaged in excavation (i.e. V) lead to ignition. The distributions of the incidents by ignition and the failure mode are shown in Fig. 2.18. This figure clearly shows that the likelihood of ignition is very small (about 3%) in leak incidents and about 10% in puncture incidents. However, the likelihood of ignition in rupture incidents is significant (about 30%).

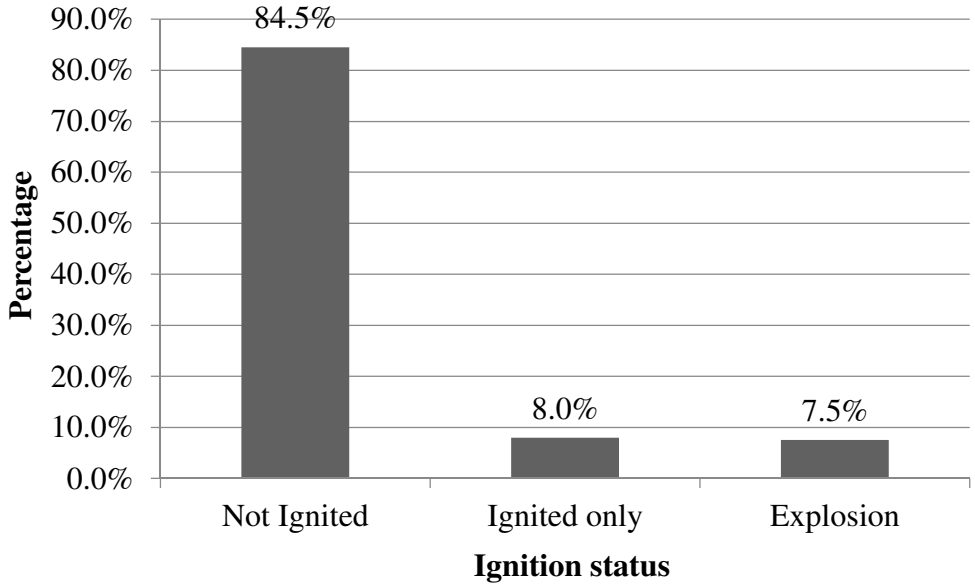

Figure 2.16 Distribution of incidents by ignition

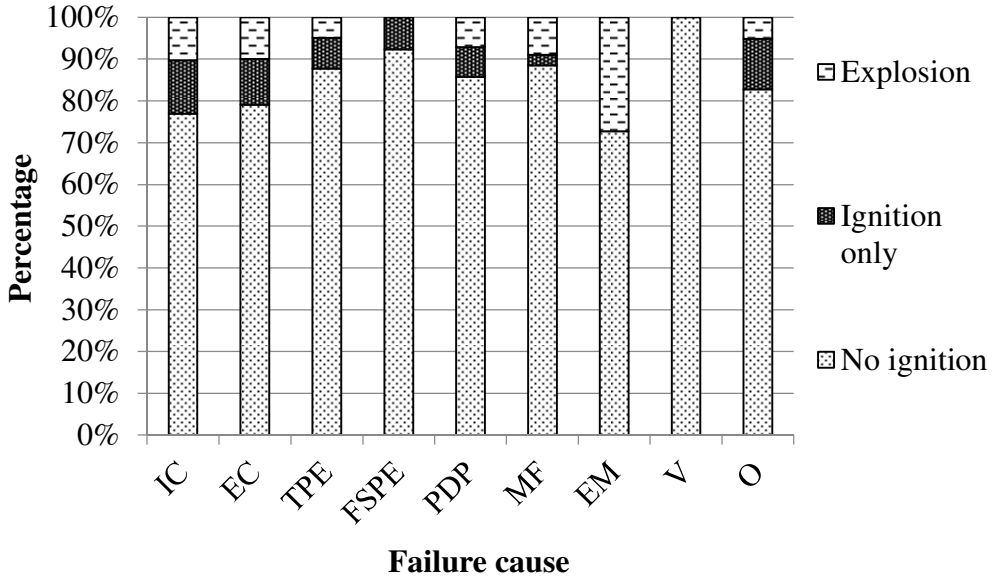

Figure 2.17 Distribution of incidents by ignition and failure cause

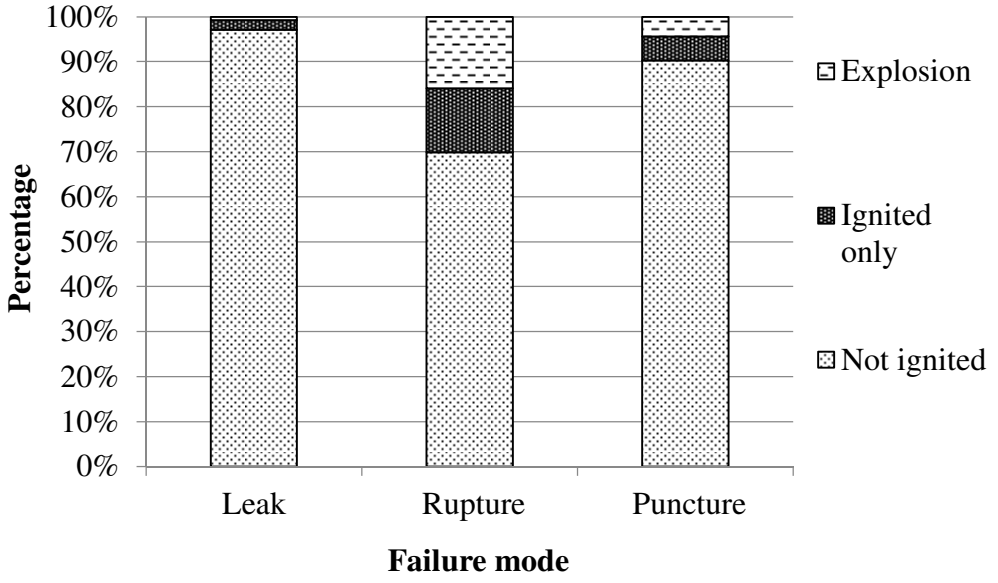

Figure 2.18 Distribution of incidents by ignition and failure mode

2.3.3.4 Distribution of injuries and fatalities

The most severe consequences associated with an ignited failure of a gas transmission pipeline are the safety implications for the population in the immediate vicinity of the

pipeline. The 464 pipe-related incidents having occurred between 2002 and 2013 caused a total of 16 fatalities and 75 injuries. The breakdowns of the fatalities and injuries by the failure cause are shown in Fig. 2.19. This figure indicates that three failure causes, i.e. MF, TPE and EC, are responsible for all the fatalities and that five failure causes, i.e. MF, TPE, EC, FSPE and PDP, are responsible for all the injuries. It should be noted that the fatalities (8) and injuries (51) associated with MF all come from one single incident: the explosion of a gas pipeline in San Bruno, California in 2010.

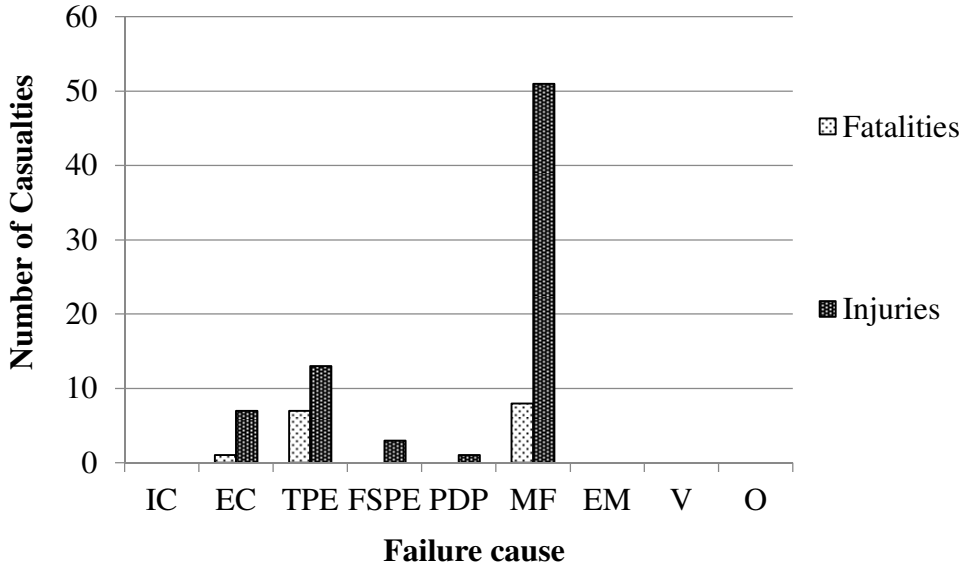

Figure 2.19 Breakdown of fatalities and injuries by failure cause

Given that the potential casualties caused by an incident is correlated with the population density in the vicinity of the pipeline, the breakdowns of the fatalities and injuries by the location class are shown in Fig. 2.20. Note that the fatalities and injuries in Class 3 all come from the San Bruno incident in 2010. All the other fatalities and injuries are due to incidents on Class 1 pipelines except for one injury due to an incident on a Class 2 pipeline. The breakdowns of the fatalities and injuries by the failure mode are shown in Fig. 2.21. The figure shows that 75 and 83% of the fatalities and injuries, respectively, were caused by rupture incidents. The PHMSA database further categories the fatalities and injuries resulting from a given incident into three groups: employees, non-employee

contractors and general public. Employees are defined as operator employees and contractor employees working for the operator, while non-employee contractors are employees of the third-party contractors. The breakdowns of the fatalities and injuries by their affiliations are shown in Fig. 2.22. The figure indicates that the majority of the fatalities and injuries were the general public.

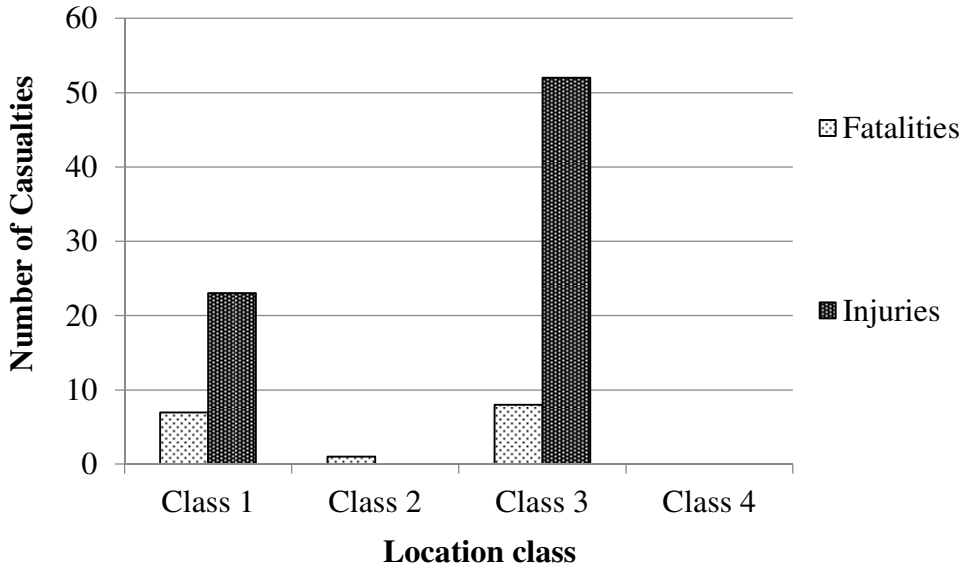

Figure 2.20 Breakdown of fatalities and injuries by location class

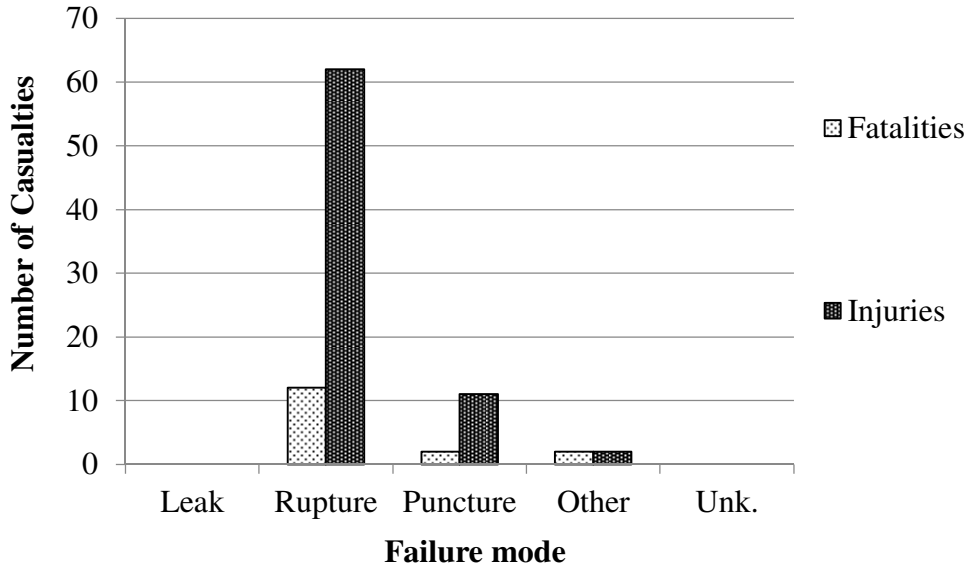

Figure 2.21 Breakdown of fatalities and injuries by failure mode

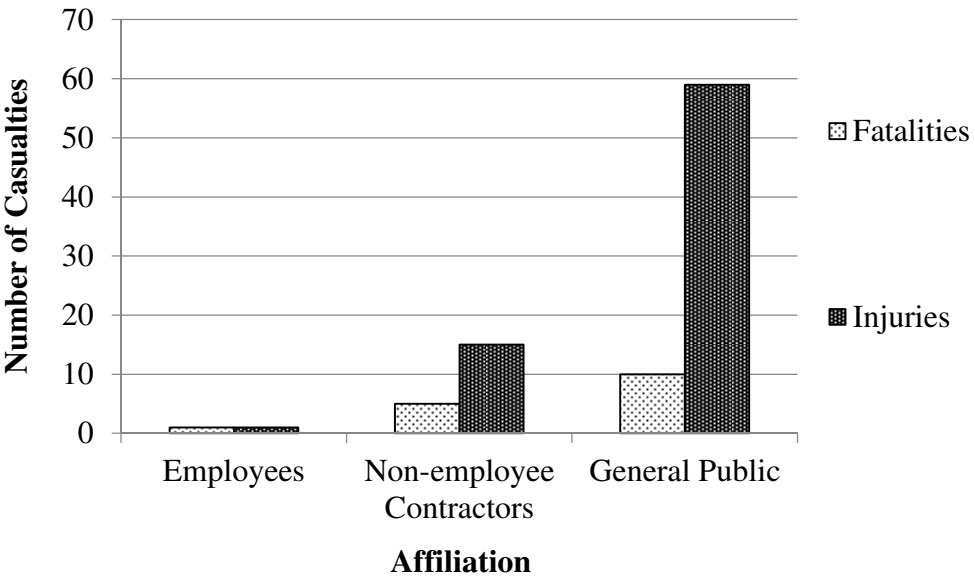

Figure 2.22 Distribution of fatalities and injuries by affiliation

2.4 Analyses of Rupture Rate

2.4.1 General

Given the incident and mileage data, the incident rate, i.e. the number of incidents per km per year can be evaluated. The significance of the incident rate is two-fold. First, it can be used as a basis for comparing the likelihoods of failure for pipelines with different attributes, if the rate is evaluated from the corresponding length of the pipeline. Second, the incident rate can be used as the annual probability of failure in the quantitative risk assessment of the pipeline in lieu of the probability of failure evaluated from more detailed analyses (e.g. the structural reliability analysis).

In this study, only the rate of the rupture incident was analyzed. This is based on two considerations. First, given the reporting criteria associated with PHMSA incident data and severity of a typical rupture incident, it can be inferred that most, if not all, of the ruptures were reported to PHMSA. On the other hand, the number of leaks or punctures that did not meet the reporting criteria may be significant compared with the number of reported leaks and punctures. Therefore, the rupture rate evaluated using the PHMSA database is believed to be representative of the actual rupture rate. Second, the consequences associated with ruptures are far more severe than those associated with leaks and punctures. This is evident from the results presented in Section 2.3.3.3 and 2.3.3.4, which show that most leaks (about 97%) and punctures (about 90%) did not result in ignition and that the majority of fatalities and injuries (75% and 83%, respectively) were due to ruptures. Therefore, the rupture rate is much more relevant to the pipeline risk assessment than the leak and puncture rates. The analysis of the rupture rate is presented in the following sections.

2.4.2 Rupture rates by failure cause and year of occurrence

The average rate of rupture between 2002 and 2013, R, due to all failure causes combined was calculated to be 3.1×10^{-5} /km-year using the following equation:

$$R = \frac{1}{12}\sum_{i=1}^{12}\frac{N_i}{L_i} \tag{2.2}$$

where N_i is the number of ruptures due to all failure causes occurring in the i^{th} year (i = 1 for year 2002), and L_i (km) is the overall length of the pipelines in the i^{th} year (see Fig. 2.1). Equation (2.2) was also used to evaluate the 12-year average rate of rupture due to the individual failure cause by replacing N_i with the number of ruptures due to the particular failure cause. The calculated rupture rates are shown in Fig. 2.23. As shown in the figure, the rupture rates due to TPE, MF, EC and IC equal 4.6×10^{-6}, 4.7×10^{-6}, 1.0×10^{-5} and 3.5×10^{-6} per km-year, respectively. The rupture rate due to the four causes combined equals 2.3×10^{-5} per km-year, which is about 74% of the rupture rate (3.1×10^{-5} per km-year) due to all failure causes combined. Figure 2.23 indicates that EC is the leading cause for ruptures of onshore gas transmission pipelines in the US between 2002 and 2013. The rupture rates due to TPE and MF, respectively, are about half of the rupture rate due to EC. Note that the rupture rate due to EC and IC combined, which equals 1.35×10^{-5} per km-year, is substantially smaller than the incident rate due to corrosion (e.g. 8.70×10^{-5} per km-year for coated pipes) obtained by Golub et al. (1996). The rupture rate due to EC is close to the incident rate due to external corrosion for CC pipelines (i.e. 9.69×10^{-6} per km-year) obtained by Kiefner et al.

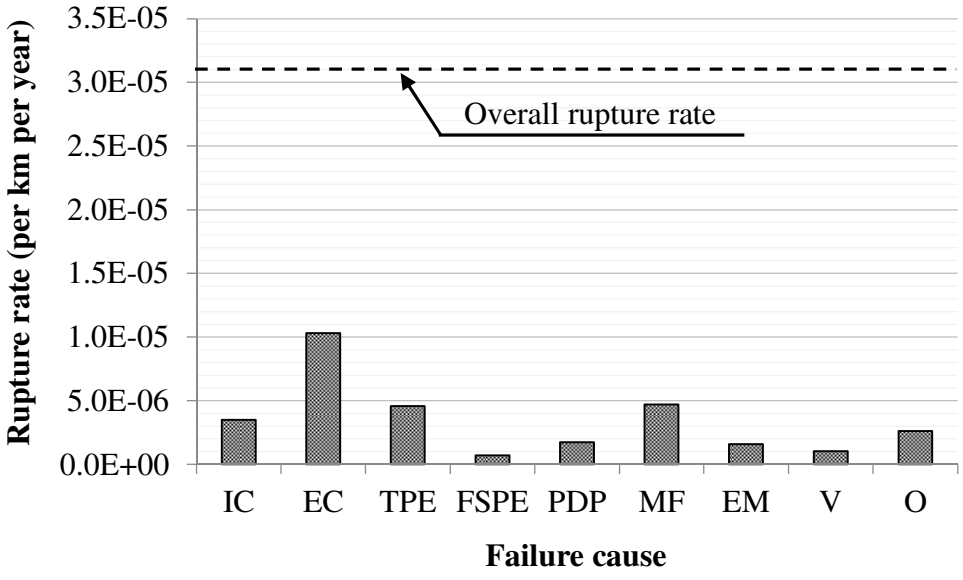

Figure 2.23 Distribution of rupture rates by failure cause

The rupture rates corresponding to all failure causes combined as well as corresponding to TPE, EC, MF and IC individually were evaluated for each year between 2002 and 2013. The results are shown in Fig. 2.24. Furthermore, the three-year moving average rupture rates were evaluated. Note that the moving average at a given year *Y* was calculated as the average of the rupture rates for years *Y*, *Y* - 1 and *Y* - 2. Therefore, the moving average starts at year 2004 in Fig. 2.25. The figure shows that the three-year moving average rupture rate due to all failure causes combined did not change much with time, although there appears to be a decreasing trend in the moving average rate since 2009. There is a clear decreasing trend in the moving average rate due to TPE between 2007 and 2011, and the rate has remained practically unchanged since 2011. The moving average rupture rates due to EC and MF appear to generally decrease and increase, respectively, since 2009. It is interesting to note that the variation pattern of the three-year moving average rupture rate corresponding to EC is consistent with that corresponding to IC.

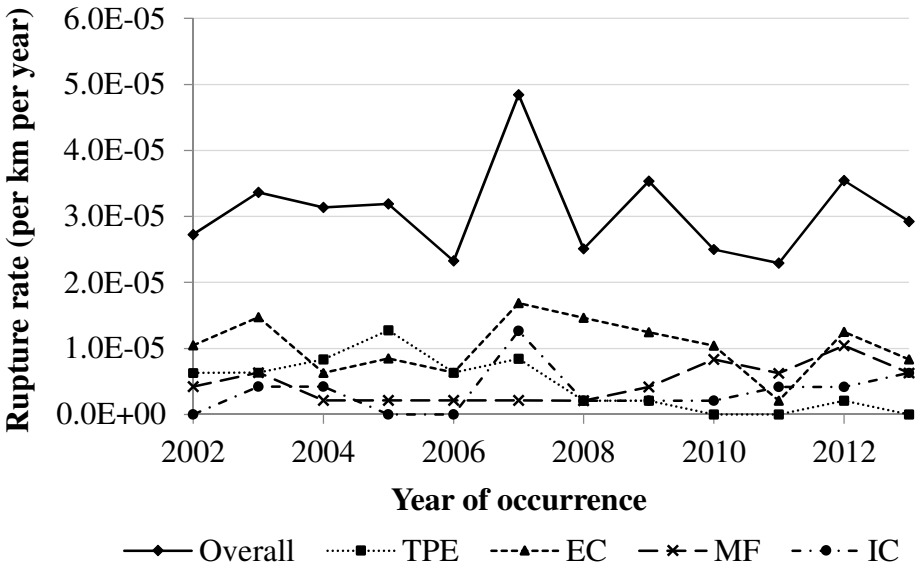

Figure 2.24 Rupture rates by year of occurrence

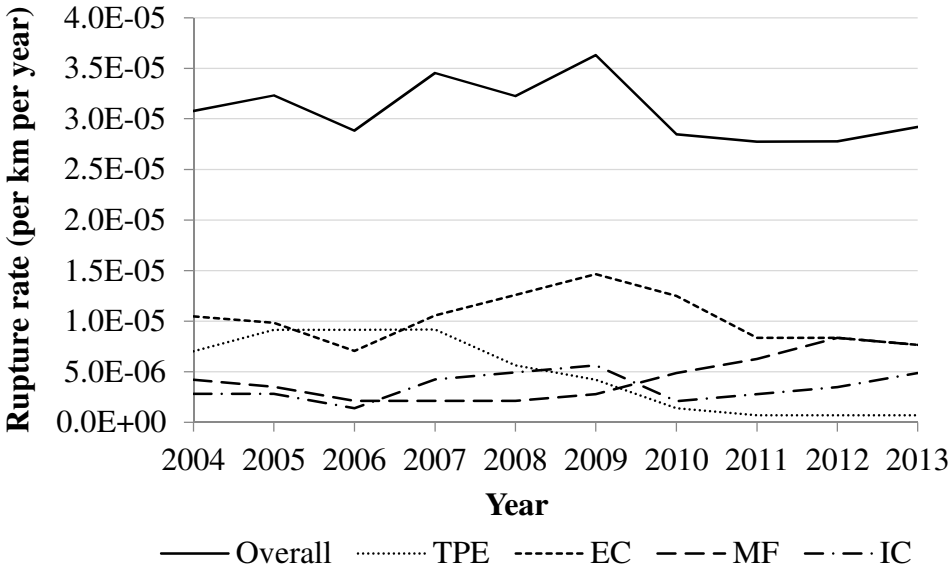

Figure 2.25 Three-year moving average rupture rates from 2004 to 2013

2.4.3 Rupture rates by pipeline attributes

The average rupture rate between 2002 and 2013 due to all failure causes combined for pipelines with a given attribute (e.g. diameter, location class or year of installation) was evaluated using the following generic equation:

$$R_{\bullet} = \frac{1}{n}\sum_{i=1}^{n}\frac{N_{i\bullet}}{L_{i\bullet}} \tag{2.3}$$

where $R_{\bullet}$ is the rupture rate for pipelines with a given attribute denoted by a generic symbol •; $N_{i\bullet}$ is the number of ruptures occurring on pipelines with attribute • in the i^{th} year; $L_{i\bullet}$ (km) is the corresponding length of pipelines with attribute • in the i^{th} year, and n is the total number of years for which the rupture and mileage data corresponding to a specific attribute are available. Note that n equals 12 in most cases; however, n equals 4 for evaluating the rupture rate for pipelines installed in the 2010s.

The rupture rates of pipelines with different diameters are shown in Fig. 2.26. The figure shows that the rupture rates corresponding to four diameter ranges, i.e. $d \leq 4$, $4 < d \leq 10$,

$20 < d \leq 28$ and $d > 28$ inches, are similar and markedly lower than the rupture rate corresponding to $10 < d \leq 20$ inches.

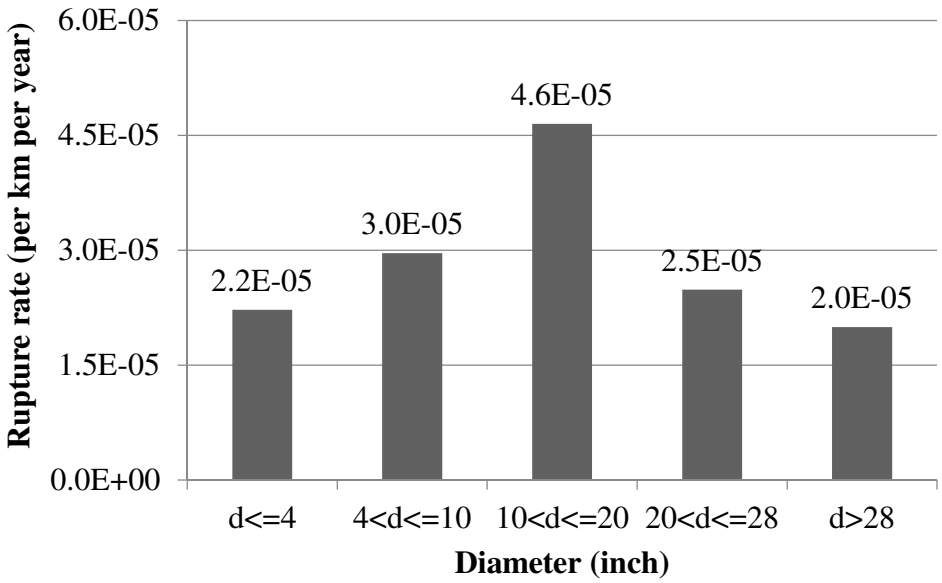

Figure 2.26 Rupture rates by diameter

The rupture rates due to TPE, EC, MF and IC for different diameter ranges were further evaluated and are compared in Fig. 2.27. The figure indicates that the TPE-caused rupture rates for small-to-medium diameter pipelines ($4 < d \leq 20$ inches) is much higher than those for pipelines with $d \leq 4$ and $d > 20$ inches. The EC-caused rupture rates for $10 < d \leq 20$ and $20 < d \leq 28$ inches are markedly higher than those for the rest of the diameter ranges. The MF-caused rupture rate is the highest for pipelines with $10 < d \leq 20$ inches. For median- and large-diameter pipelines ($d > 10$ inches), the EC-caused rupture rates are markedly higher than those due to TPE, MF and IC, which suggests that EC is the most common cause for ruptures of such pipelines.

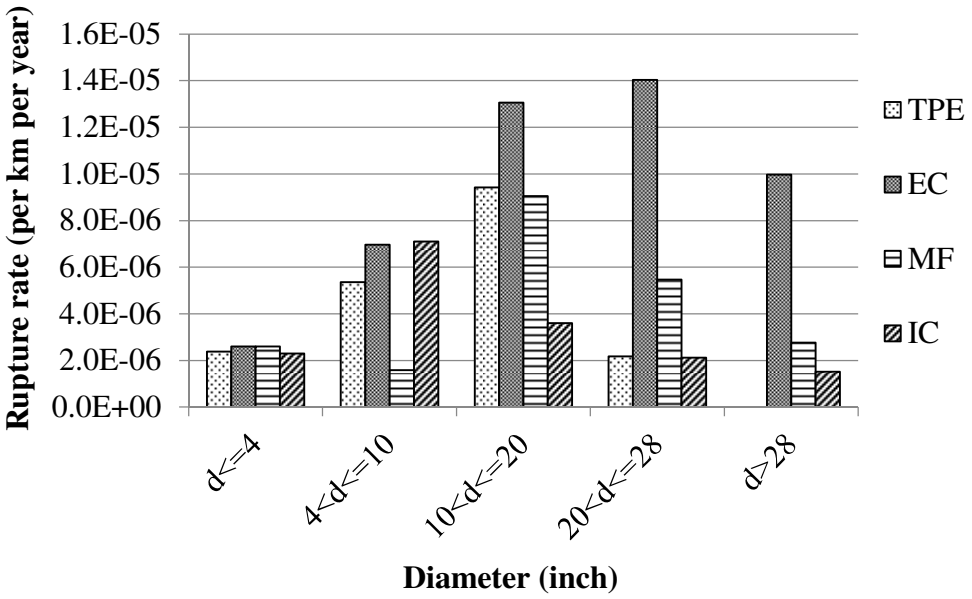

Figure 2.27 Rupture rates due to TPE, EC, MF and IC by diameter

The average rupture rates due to all failure causes combined for pipelines with different years of installation are shown in Fig. 2.28. The figure clearly shows that the rupture rates for newer pipelines are lower than those for older pipelines, except for one anomaly whereby the rupture rate for pipelines installed in the 2010s is markedly higher than those for pipelines installed in 1980s, 1990s and 2000s. This is due to the fact that the total length of the pipelines installed in the 2010s is small compared with the lengths of the pipelines installed in other periods. For example, the total lengths of the pipelines installed in the 2010s are 3,201, 8,084, 11,092 and 13,910 km in 2010, 2011, 2012 and 2013, respectively, whereas the total lengths of the pipelines installed in the 2000s are 46,380, 46,821, 47,581 and 47,547 km in 2010, 2011, 2012 and 2013, respectively. In fact, only one rupture occurred on pipelines installed in the 2010s between 2010 and 2013.

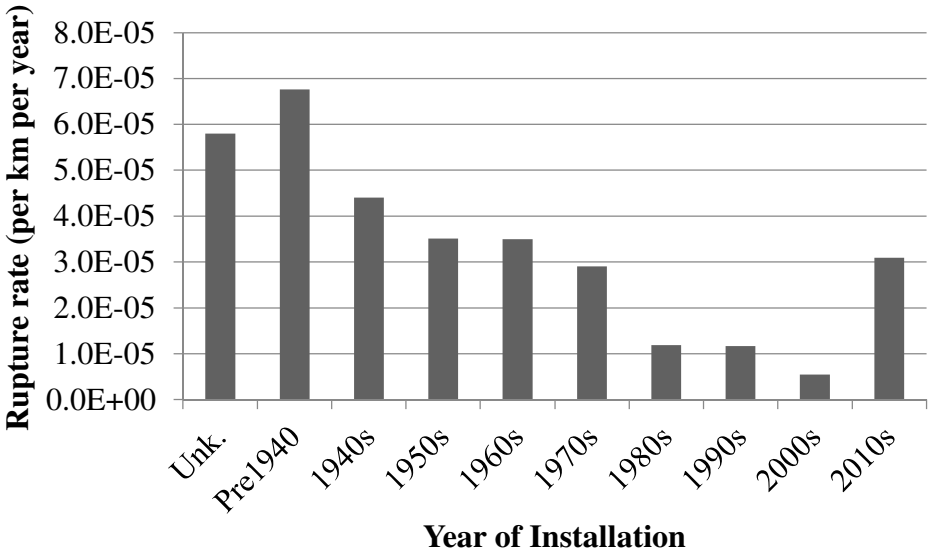

Figure 2.28 Distribution of rupture rates by year of installation

The rupture rates due to TPE, EC, MF and IC for pipelines with different years of installation are compared in Fig. 2.29. The figure shows that the EC-caused rupture rate increases in general as the pipeline age increases; however, there is no strong correlation between the IC-caused rupture rate and pipeline age. Note that the TPE-caused rupture rate generally increases as the pipeline age increases. One hypothesis to explain this phenomenon is that the actual locations of older pipelines may not be as clearly indicated as those of newer pipelines, which makes older pipelines more susceptible to third-party excavation activities. This may also explain that the TPE-caused rupture rate for pipelines with unknown years of installation is the highest, as such pipelines are mostly likely to have incomplete records for their locations, making them most susceptible to third-party excavations. MF-caused rupture rates for older pipelines are basically higher than those for newer pipelines except pipelines installed in 2010s, which is due to the relative short length of such pipelines as explained in the previous paragraph. Finally, Fig. 2.29 indicates that EC is the leading cause for rupture for all pipelines installed in the 1960s or earlier.

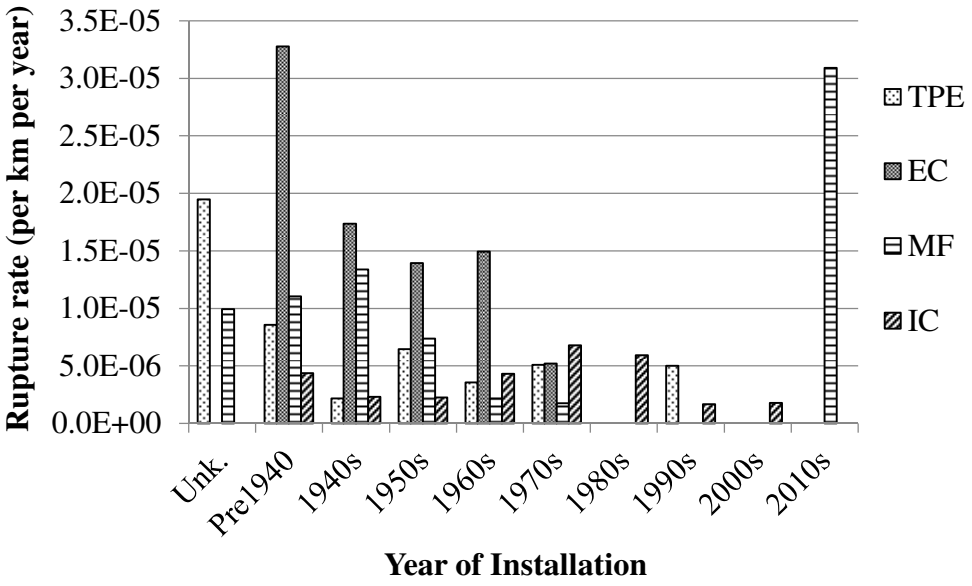

Figure 2.29 Rupture rates due to TPE, EC, MF and IC by year of installation

The rupture rates due to all failure causes combined for pipelines in different classes are shown in Fig. 2.30. The figure shows that the rupture rates for Classes 1, 2 and 3 pipelines are somewhat similar.

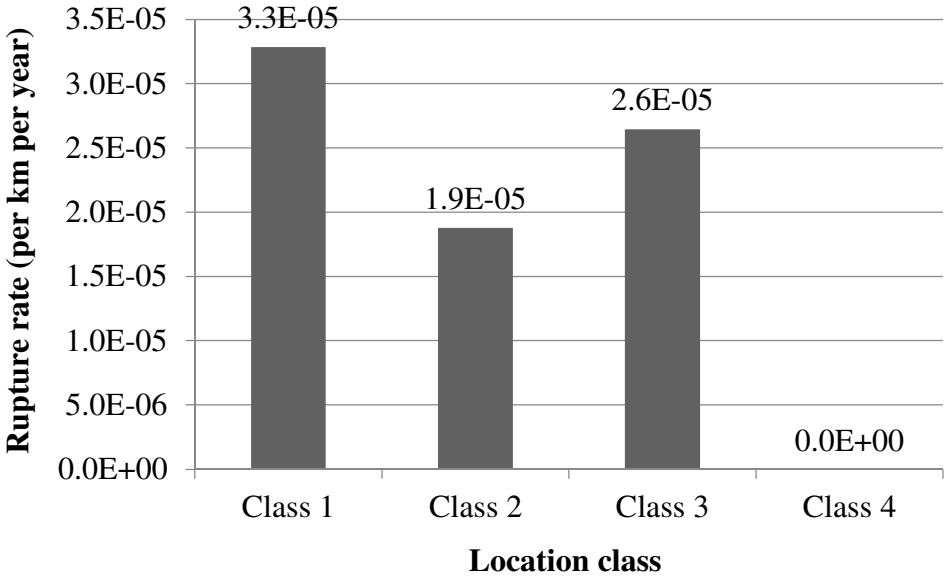

Figure 2.30 Distribution of rupture rates by location class

The rupture rates due to TPE, EC, MF and IC for pipelines with different location classes are compared in Fig. 2.31. As the relatively high population density in Class 3 areas implies more third-party excavation activities, it is not entirely unexpected that the TPE-caused rupture rate for Class 3 pipelines is markedly higher than those for Class 2 and Class 1 pipelines. This however suggests that the safety factor incorporated in the design of the wall thickness for Class 3 pipelines may not be adequate from the perspective of preventing the third-party excavation damage.

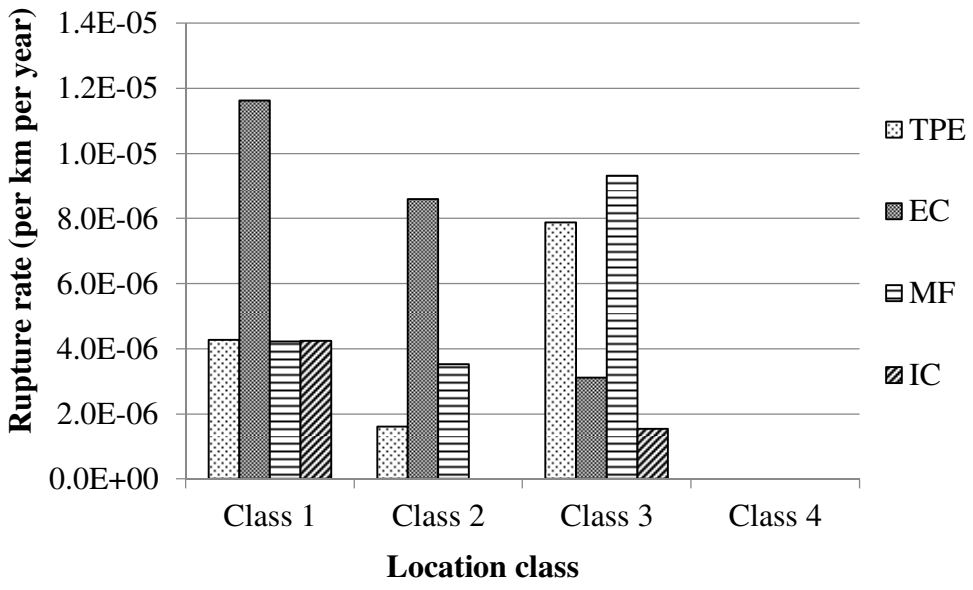

Figure 2.31 Rupture rates due to TPE, EC, MF and IC by location class

2.5 Conclusions

In this study, we carried out statistical analyses of the mileage and pipe-related incidents corresponding to onshore gas transmission pipelines in the United States between 2002 and 2013 obtained from the PHMSA database. The incident data for the periods of 2002-2009 and 2010-2013 were aggregated by either the failure cause or failure mode. The set of failure causes adopted in this study included the internal and external corrosions (IC and EC), third-party excavation (TPE), material failure (MF), first- and second-party excavation (FSPE), previously damage pipe (PDP), vehicle not engaged in excavation (V) and other (O). The set of failure modes adopted in this study included leak, puncture,

rupture and other. The mileage and incident data were used to evaluate the rate of rupture incidents per km per year for onshore gas transmission pipelines. The following are the main findings of the analysis.

1. The total length of the onshore gas transmission pipelines in the US varied between about 470,000 and 480,000 km from 2002 to 2013, and remained at around 480,000 km since 2009. About 97% of the pipelines are steel pipelines with both the coating and cathodic protection. As of 2013, about 60% of the pipelines were more than 45 years old.

2. Class 1 pipelines account for approximately 80% of the total length; Class 2 and Class 3 pipelines, respectively, account for about 10% of the total length, and the length of Class 4 pipelines is negligibly small.

3. TPE, EC, MF and IC are the four most common causes for the pipe-related incidents, responsible for over 75% of a total of 464 incidents between 2002 and 2013. About 50% of the incidents were caused by TPE and EC. The proportion of corrosion-caused incidents in this study is about 32% and markedly larger than the proportions of corrosion-caused incidents obtained by Golub et al. in 1996 and Kiefner et al. in 2001. Approximately 80% of the TPE- and 85% of the IC-caused incidents occurred on pipelines with small or medium diameters ($4 < d \leq 20$ inches) whereas about 79% of the EC- and 87% of the MF-caused incidents occurred on pipelines with medium or large diameters ($d > 10$ inches).

4. Rupture is the most common failure mode, with 38% of the incidents resulting in ruptures. About 30% and 20% of the incidents resulted in leaks and punctures, respectively. Just over half of EC- and IC-caused incidents resulted in ruptures; 60% and 22% of TPE-caused incidents resulted in punctures and ruptures, respectively, and 55% and 35% of MF-caused incidents resulted in leaks and ruptures, respectively.

5. The likelihood of ignition given a leak, puncture or rupture approximately equals 3, 10 or 30%, respectively. Rupture incidents are responsible for 75 and 83%, respectively, of a total of 16 fatalities and 75 injuries resulting from the 464 pipe-related incidents between 2002 and 2013.

6. The 12-year average rupture rate equals 3.1×10^{-5} /km-year due to all failure causes combined, and 2.3×10^{-5} /km-year due to TPE, EC, MF and IC combined. The rupture rate due to EC and IC combined equals 1.35×10^{-5} /km-year and is notably smaller than the incident rate due to corrosion (e.g. 8.70×10^{-5} per km-year for coated pipes) obtained by Golub et al. (1996). EC is the leading cause for rupture: the EC-caused rupture rate equals 1.0×10^{-5} /km-year and is about twice the rupture rate due to TPE or MF. The rupture rate due to EC is close to the incident rate due to corrosion for CC pipelines (i.e. 9.69×10^{-6} per km-year) obtained by Kiefner et al. in 2001. Furthermore, EC is the leading cause for rupture for all pipelines installed in the 1960s or earlier.

7. The three-year moving average rupture rate due to TPE gradually decreased between 2007 and 2011 and remained almost unchanged since 2011. There appears to be decreasing and increasing trends, respectively, in the three-year moving average rupture rates due to EC and MF since 2009.

8. The TPE-caused rupture rate for Class 3 pipelines is markedly higher than those for Class 1 and Class 2 pipelines. This suggests that the safety factor prescribed for the design of Class 3 pipelines may not be adequate in terms of protecting the pipelines from the third-party excavation damage.

9. It is suggested that the PHMSA pipeline mileage data include a more refined data structure to allow the breakdown of the mileage by more than one pipeline attributes and evaluation of the rupture rates for pipelines with different attributes.

References

ASME 2013. ASME B31.8: Gas transmission and distribution piping systems. The American Society of Mechanical Engineers, Three Park Avenue, New York, NY.

USOFR (US Office of the Federal Register). 2013. Code of Federal Regulations (CFR). 2013. Title 49: Transportation, parts 178 to 199, US Government Printing Office, Washington, DC 20402.

Golub, E., Greenfeld, J., Dresnack, R., Griffis, F.H. and Pignataro, L.J. 1996. Pipeline accident effects for gas transmission pipelines. DTRS 56-94-C-0006, National Technical Information Service, Springfield, Virginia 22161.

Kiefner, J.F., Mesloh, R.E. and Kiefner, B.A. 2001. Analysis of DOT reportable incidents for gas transmission and gathering system pipelines, 1985 through 1997. L51830e, Technical Toolboxes, Inc., Houston, Texas 77098.

Chapter 3

Development of Probability of Ignition Model for Ruptures of Onshore Gas Transmission Pipelines

3.1 Introduction

In the US and Canada, onshore transmission pipelines are the most common means to transport large quantity of natural gas from processing plants in gas producing regions to distribution centres in high-consumption regions. Failures, defined as the loss of pressure containment, of these pipelines do occur, albeit infrequently, due to various causes such as the third-party excavation activities, internal/external corrosion and ground movement. Three failure modes are generally associated with onshore pipelines, namely the small or pinhole leak, large leak (or puncture) and full-bore rupture (Nessim et al. 2009). A given failure may or may not lead to ignition of the released gas. In terms of human safety and property damage, the consequences associated with non-ignited failures and ignited small/large leaks are in general low (Acton and Baldwin 2008; Nessim et al. 2009). However, the consequences of ignited ruptures of gas pipelines can be extremely severe, as evident from such well-known past failures as the Carlsbad, New Mexico incident in 2000 (NTSB 2003) and San Bruno, California incident in 2010 (NTSB 2011). Therefore, an important task in the quantitative risk assessment of onshore gas transmission pipelines is to estimate the probability of ignition (POI) given rupture.

Acton et al. (2002) reviewed the pipeline incident data obtained from onshore gas transmission pipeline operators in Europe and Canada, and investigated the relationship between POI and the product of the internal pressure at the time of the incident (p) and square of the outside diameter (d^2) of the pipeline, whereby pd^2 is directly related to the initial gas outflow from a rupture. The authors grouped pipelines into different ranges of pd^2 values and calculated POI within a given range of pd^2 values as the proportion of the number of ignited incidents to the total number of incidents within the range. The POI values were observed to increase approximately linearly with the average pd^2 values

corresponding to different pd^2 ranges. The authors therefore proposed a simple POI model for rupture as follows:

$$\text{POI} = A + Bpd^2 \leq \text{POI}_{max} \tag{3.1}$$

where A and B are the model parameters and can be evaluated from the least squares-based simple linear regression analysis, and POI_{max} is an upper bound probability of ignition. Acton et al. suggested POI_{max} to be set at 0.8, but did not report the values of A and B.

Acton and Baldwin (2008) reported the values of A, B and POI_{max} in Eq. (3.1) based on the onshore gas transmission pipeline incident data obtained from the PIPESAFE Group (consisting of several gas transmission pipeline companies in Europe and Canada) and the pipeline incident database administered by the Pipeline and Hazardous Material Safety Administration (PHMSA) of the United States Department of Transportation. Based on the rupture incident data between 1970 and 1996 obtained from the PIPESAFE Group, A, B and POI_{max} were evaluated to be 0.0725, 0.0151 and 0.8, respectively. Based on the PIPESAFE rupture data between 1970 and 2004, the values of A, B and POI_{max} were reported to be 0.0584, 0.0160 and 0.83, respectively. Finally, based on the combined PIPESAFE rupture data between 1970 and 2004 and PHMSA rupture data between 2002 and 2007, the values of A, B and POI_{max} were reported to be 0.0555, 0.0137 and 0.81, respectively. Note that the units of p and d in Eq. (3.1) are bar (1 bar = 0.1 MPa) and meter, respectively, corresponding to the aforementioned B values.

There are several drawbacks associated with the POI model given by Eq. (3.1). First, the model parameters are evaluated by grouping the incident data into ranges of pd^2 values. The sensitivity of the model parameters to the grouping criterion has not been investigated. Second, the model is not naturally bounded by zero and unity as required by the nature of probability. The lack of the upper bound of unity is in particular problematic; therefore, a somewhat arbitrary upper bound (POI_{max}) is included in the model. Finally, the least squares-based simple linear regression analysis used to fit the POI model is predicated on the condition that the difference between the observed and

predicted outcomes (i.e. error) is normally distributed with a constant variance (Hosmer et al. 2013). However, such a condition is violated for the POI model because the observed outcome of the data used in the fitting is of the binary nature (Hosmer et al. 2013), i.e. either ignition or non-ignition for a given incident.

The objective of the study reported in this chapter was to develop a new POI model that overcomes the drawbacks of the POI model given by Eq. (3.1). To this end, both the logistic and log-logistic POI models were proposed. The maximum likelihood method was employed to evaluate the model parameters based on the onshore gas transmission pipeline rupture incident data between 2002 and 2014 included in the PHMSA database. The PIPESAFE rupture incident data reported by Acton and Baldwin (2008) were used to validate the proposed POI model. The new POI model will facilitate the risk assessment of onshore natural gas transmission pipelines.

The rest of this chapter is organized as follows. Section 3.2 presents a brief overview of the PHMSA incident database and exploratory analyses of the PHMSA incident data selected for this study. The evaluation of the parameters of the proposed POI model using the maximum likelihood method is described in Section 3.3. The confidence interval associated with the proposed model is also presented in Section 3.3. The validation of the model is presented in Section 3.4, followed by summary and conclusions in Section 3.5.

3.2 PHMSA Pipeline Incident Data and Exploratory Data Analysis

Since 1970, operators of oil and gas pipelines regulated by PHMSA have been required to submit incident reports to PHMSA within 30 days of the occurrence of incidents that meet the reporting criteria specified in the Code of Federal Regulations (CFR) Parts 191 and 195 (USOFR 2013). PHMSA's incident report includes information such as the cause (e.g. third-party excavation, external corrosion, earth movement, etc.) of the incident as well as the basic attributes (e.g. diameter, maximum allowable operating pressure, internal pressure at the time of the incident, etc.) and failure mode (i.e. leak,

puncture or rupture) of the pipeline involved in the incident. The reported incidents were stored in the PHMSA pipeline incident database, which can be accessed from http://www.phmsa.dot.gov/pipeline/library/data-stats. Starting in 2002, whether an incident involved ignition was included in the incident report, which makes it feasible to develop a POI model based on the PHMSA incident data dated in or after 2002.

The PHMSA incident data between 2002 and 2014 were examined to select the appropriate data for the present study based on two criteria: 1) the incidents occurred on onshore natural gas transmission pipelines, and 2) the pipelines failed by full-bore rupture. A total of 188 rupture incidents were identified as a result, 59 of them being ignited incidents. The diameters of the pipelines involved in the incidents range from 13.7 to 914.4 mm; the maximum allowable operating pressures range from 1.0 to 20.7 MPa, and the internal pressures at times of incidents range from 0.3 to 14.6 MPa. Detailed information about the data is included in Appendix A.

In light of Eq. (3.1), the potential correlation between POI and pd^2 (MPa-mm^2) for the selected data set was examined first. To this end, ten pd^2 values were selected to divide the 188 data points into ten groups, with each group consisting of approximately 19 data points. For each group, POI was then computed as the ratio of the number of ignited incidents to the number of all incidents in the group, and the average pd^2 value for all the incidents in the group was also evaluated. Table 3.1 summarizes the grouped data.

Table 3.1 Estimated POI with pd^2 for PHMSA rupture incident data

Group No.	pd^2 Range ($\times 10^5$ MPa-mm^2)	No. of Incidents	No. of Ignited Incidents	Mean pd^2 for Incidents ($\times 10^5$ MPa-mm^2)	POI
1	≤ 0.8	19	1	0.5	5.3%
2	(0.8, 2.3]	19	0	1.6	0.0%
3	(2.3,3.2]	19	3	2.8	15.8%
4	(3.2, 4.9]	19	2	4.3	10.5%
5	(4.9, 8.1]	19	6	6.2	31.6%
6	(8.1, 10.6]	18	5	9.6	27.8%
7	(10.6, 15.5]	19	8	12.9	42.1%
8	(15.5, 20.1]	19	8	17.8	42.1%
9	(20.1, 35.8]	19	11	25.8	57.9%
10	> 35.8	18	13	43.8	72.2%

The POI values for the ten groups are plotted against the corresponding average pd^2 values in Fig. 3.1. The figure suggests that there is a strong correlation between POI and pd^2: the correlation coefficient between the sets of POI and pd^2 values equals 0.94. This observation agrees with that made by Acton et al. (2002) and confirms the suitability of pd^2 as a predicator in the POI model.

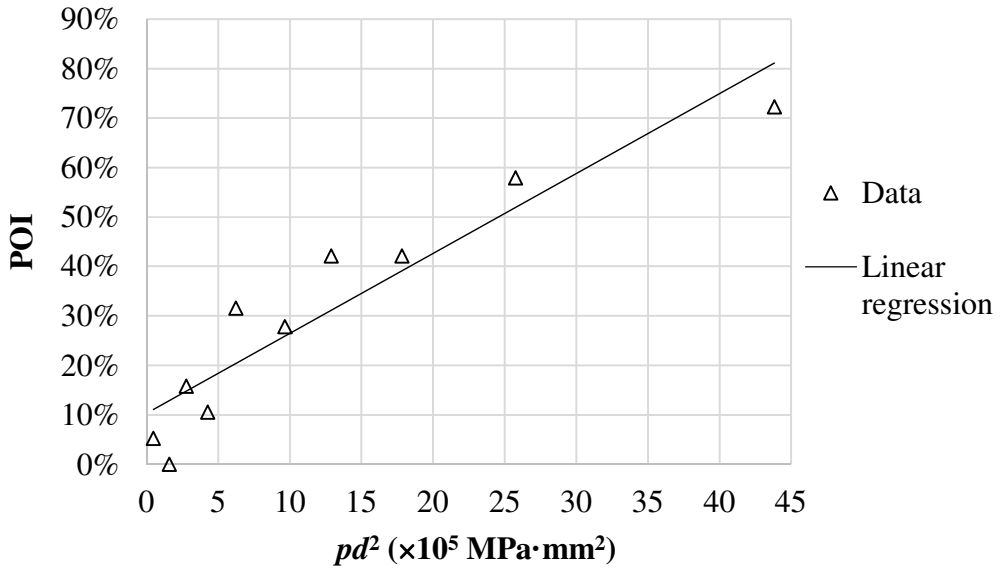

Figure 3.1 POI vs. pd^2 for the PHMSA rupture data

The potential correlation between POI and the location class of the ruptured pipeline was also investigated. In the US, a natural gas pipeline is assigned a location class that characterizes the population density in the vicinity of the pipeline. According to ASME B31.8 (ASME 2013) and Part 191, Title 49 of CFR (USOFR 2013), there are four location classes for gas pipelines, namely Class 1, Class 2, Class 3 and Class 4. The Class 1 represents sparsely populated areas such as wasteland, deserts and farmland; the Class 2 reflects fringe areas around cities and towns, industrial areas, ranch or country estates, etc.; the Class 3 reflects areas such as suburban housing developments, shopping centres, residential areas, etc., and the Class 4 represents city centres where multistory buildings (defined as having four or more floors above ground) are prevalent and traffic is heavy. A higher population density implies the presence of more potential ignition sources; therefore, it is hypothesized that POI for ruptures of pipelines of higher location classes is greater than that for pipelines of lower location classes.

The 188 data points were grouped by their corresponding location classes. POI for each location class was evaluated as the ratio of the number of ignited ruptures to the number of all ruptures in the class. The results are shown in Table 3.2. For comparison, the average pd^2 values for all the ruptures in different location classes are also shown in the

table. Table 3.2 indicates that more than 80% of all ruptures occurred on Class 1 pipelines and no rupture occurred on Class 4 pipelines. This is consistent with the fact that approximately 80% of the onshore gas transmission pipelines in the US are Class 1 pipelines and the percentage of Class 4 pipelines is negligibly small (see Chapter 2). The table also indicates that the trend in POI is somewhat unclear as the location class increases: the POI for the Class 2 pipelines is the highest whereas the POI for the Class 3 pipelines is the lowest. Note that the unclear trend may be partly attributed to the small sample sizes for both Class 2 and Class 3 pipelines compared with that for Class 1 pipelines.

Table 3.2 Estimated POI with location class for rupture incidents

Group No.	1	2	3	4	5
Location Class	Class 1	Class 2	Class 3	Class 4	Unknown
No. of Incidents	156	13	18	0	1
No. of Ignited Incidents	48	6	3	0	0
POI	30.8%	46.2%	16.7%	-	0.0%
pd^2 Mean ($\times 10^5$ MPa-mm^2)	13.6	10.6	3.8	-	2.2

3.3 Probability of Ignition Model

3.3.1 Logistic and log-logistic POI models

The logistic function is widely employed in the literature to characterize the probability of a binary outcome corresponding to a set of predictors, for example, the probability of detecting a flaw with a given size associated with the non-destructive testing (Zheng and Ellingwood 1998) and the likelihood of a person with a given age suffering from a certain disease (Hosmer et al. 2013). In this study, the logistic function was adopted as a candidate POI model. Based on the results of the exploratory data analysis described in

Section 3.2, the variable pd^2 (MPa-mm^2) and the location class C_l (C_l = 1, 2, 3 or 4) were selected as the predictors in the logistic POI model, which is given by

$$\text{POI} = \frac{1}{1+e^{-\alpha_1-\alpha_2(pd^2)-\alpha_3 C_l}} \tag{3.2}$$

where α_1, α_2 and α_3 are the model parameters to be evaluated.

In addition to the logistic function, the log-logistic function (Leemans and Frosyth, 2004; Lu et al. 2014) was also considered as a candidate POI model in this study:

$$\text{POI} = \frac{1}{1+e^{-\beta_1-\beta_2 \ln(pd^2)-\beta_3 \ln C_l}} \tag{3.3}$$

where β_1, β_2 and β_3 are the corresponding model parameters. The advantage of the log-logistic model is that POI approaches zero for pd^2 close to zero, which physically makes sense.

3.3.2 Maximum likelihood estimation of model parameters

The maximum likelihood method was employed to evaluate the parameters α_1, α_2, α_3, β_1, β_2 and β_3 in Eqs. (3.2) and (3.3) based on the 188 data points collected from the PHMSA incident database as described in Section 3.2. Let **D** denote a set of n rupture incident data**.** If ignition occurred in the i^{th} incident (i = 1, 2, ..., n), let λ_i = 1; otherwise, let λ_i = 0. Further let $\boldsymbol{\theta}$ denote the vector of unknown parameters in the POI model to be evaluated from **D**, i.e. $\boldsymbol{\theta}$ = (α_1, α_2, α_3) and (β_1, β_2, β_3) for the logistic and log-logistic POI models, respectively. If the incident data are assumed to be mutually independent, the likelihood of the data as a function of $\boldsymbol{\theta}$, $L(\boldsymbol{\theta}|\mathbf{D})$, is given by (Hosmer et al. 2013)

$$L(\boldsymbol{\theta}|\mathbf{D}) = \prod_{i=1}^{n} (\text{POI}_i)^{\lambda_i} \cdot (1 - \text{POI}_i)^{1-\lambda_i} \tag{3.4}$$

where POI_i denotes the value of POI for the i^{th} data point and can be obtained by substituting the corresponding value of pd^2 and C_l $(pd^2)_i$ and C_{li} into Eq. (3.2) and Eq. (3.3) for the logistic and log-logistic POI model, respectively. The maximum likelihood estimators of $\boldsymbol{\theta}$ are the values of $\boldsymbol{\theta}$ that maximize Eq. (3.4). It is preferable to maximize

the logarithmic of the likelihood function, i.e. log-likelihood function, as opposed to the likelihood function itself. The log-likelihood function corresponding to Eq. (3.4) is given by

$$ln\big(L(\boldsymbol{\theta}|\boldsymbol{D})\big) = \sum_{i=1}^{n} \lambda_i ln(POI_i) + \sum_{i=1}^{n} (1-\lambda_i) ln(1-POI_i) \tag{3.5}$$

An iterative procedure is needed to evaluate $\boldsymbol{\theta}$ that maximizes Eq. (3.5). In this study, the generalized linear model fitting in the general purpose statistical analysis software R was employed to compute the maximum likelihood estimators (Maindonald 2008). The results for the logistic and log-logistic POI models are summarized in Table 3.3.

It is desirable to evaluate if the maximum likelihood estimator of a given parameter is significantly different from zero, which sheds light on if pd^2 (ln(pd^2)) and C_l (ln(C_l)) are significantly related to ignition in the logistic (log-logistic) POI model. The Wald test (Hosmer et al. 2013) was adopted to carry out the significance test. Consider the logistic POI model (the Wald test for the log-logistic model follows the same procedure), the Wald test statistics, W_i, for a given parameter θ_i (i = 1, 2 or 3) is as follows:

$$W_i = \hat{\theta}_i / SE\big(\hat{\theta}_i\big) \tag{3.6}$$

where $\hat{\theta}_i$ is the maximum likelihood estimator of θ_i, and $\mathrm{SE}\big(\hat{\theta}_i\big)$ is the corresponding standard error of $\hat{\theta}_i$. For large sample sizes and under the null hypothesis that $\theta_i = 0$, W_i is a standard normal variate (Hosmer et al. 2013). To obtain an estimator of $\mathrm{SE}\big(\hat{\theta}_i\big)$, the observed Fisher information matrix, $\mathbf{I_F}$, is obtained first as the negative of the Hessian matrix of the log-likelihood function computed at the point of the maximum likelihood estimates (Carroll and Ruppert 1988):

$$\boldsymbol{I}_F = -\frac{\partial^2 ln\,(L(\boldsymbol{\theta}|\boldsymbol{D}))}{\partial\theta_i \partial\theta_j}\Big|_{\boldsymbol{\theta}=\hat{\boldsymbol{\theta}}} \; (i, j = 1, 2, 3) \tag{3.7}$$

The estimated variance-covariance matrix of $\hat{\theta}_i$ equals the inverse of the Fisher information matrix (Carroll and Ruppert 1988). Finally, the estimator of $\mathrm{SE}\big(\hat{\theta}_i\big)$ equals the square root of the corresponding diagonal element of the estimated variance-

covariance matrix. The values of $\hat{\theta}_i$ and estimator of $\mathrm{SE}(\hat{\theta}_i)$ are substituted into Eq. (3.6) to calculate a value of W_i, w_i. The null hypothesis of $\theta_i = 0$ is rejected (i.e. $\theta_i \neq 0$) if $|w_i| > \Phi^{-1}(1 - \alpha/2)$, where $\Phi^{-1}(\bullet)$ is the inverse of the standard normal distribution function, and α is the two-sided significance level. In this study, α was selected to equal 0.05, resulting in $\Phi^{-1}(1 - \alpha/2) = 1.96$.

The standard errors of the estimated parameters were obtained using the software R. The Wald test results for the logistic and log-logistic models are summarized in Table 3.3. The table shows that the absolute values of the Wald statistics for α_3 and β_3 are markedly smaller than $\Phi^{-1}(1 - \alpha/2) = 1.96$; therefore, the α_3 (β_3) is considered not significantly different from zero and C_l ($\ln(C_l)$) is not significantly related to ignition in the logistic (log-logistic) POI model.

Table 3.3 Maximum likelihood estimates for the logistic and log-logistic POI models considering the location class

Parameter	Maximum likelihood estimator	Std. Error	Wald Statistics
α_1	-2.12	0.50	-4.23
α_2	7.77×10^{-7}	1.52×10^{-7}	5.12
α_3	0.19	0.29	0.65
β_1	-16.17	2.90	-5.58
β_2	1.11	0.21	5.42
β_3	0.65	0.55	1.17

After eliminating the location class as a predictor, the logistic and log-logistic POI models are given by Eqs. (3.8) and (3.9), respectively.

$$\text{POI} = \frac{1}{1+e^{-\alpha_1-\alpha_2(pd^2)}} \tag{3.8}$$

$$\text{POI} = \frac{1}{1+e^{-\beta_1-\beta_2 \ln(pd^2)}} \tag{3.9}$$

The maximum likelihood estimators of α_1, α_2, β_1 and β_2 were evaluated to be -1.86, 7.59×10^{-7}, -15.36 and 1.06, respectively, with the corresponding standard errors equal to 0.27, 1.47×10^{-7}, 2.73 and 0.20, respectively.

3.3.3 Goodness-of-fit and confidence interval

To determine how well Eqs. (3.8) and (3.9) fit the incident data, the Hosmer-Lemeshow (HL) method was used to perform the goodness-of-fit test (Hosmer et al. 2013). The HL test involves first sorting the predicted POI values for all the data point in an ascending order and then dividing the incident data into several groups such that each group contains approximately equal number of data points. The HL test statistics, H, is then obtained from the following equation:

$$H = \sum_{i=1}^{g} \frac{(O_i - N_i\overline{\text{POI}}_i)^2}{N_i\overline{\text{POI}}_i(1-\overline{\text{POI}}_i)} \tag{3.10}$$

where g is the number of groups; O_i is the observed number of ignited incidents in the i^{th} group; N_i is total number of incidents (ignited and non-ignited) in the i^{th} group, and $\overline{\text{POI}}_i$ is the average predicted POI for the i^{th} group. Under the null hypothesis that the predicted POI is the same as the observed POI, H asymptotically follows a chi-square distribution with (g-2) degrees of freedom (Hosmer et al. 2013). For a given value of H, h, the null hypothesis is accepted if $h < {\chi^2_{g-2}}^{-1}(1-\alpha)$, where ${\chi^2_{g-2}}^{-1}(\bullet)$ denotes the inverse of the probability distribution function of a chi-square distribution with g - 2 degrees of freedom, and α is the one-sided significance level. In this study, the incident data were divided into ten groups (i.e. g = 10) and α = 0.05 was selected, resulting in ${\chi^2_{g-2}}^{-1}(1-\alpha)$ = 15.5.

The HL tests for the logistic and log-logistic POI models were carried out in R (Maindonald 2008). The results are depicted in Figs. 3.2(a) and 3.2(b), respectively. A

comparison of these two figures suggest that the log-logistic POI model fits the incident data better than the logistic POI model. This is also confirmed by the corresponding HL statistics: the h values for the logistic and log-logistic POI models equal 7.91 and 3.84, respectively. Note that both h values are less than ${\chi^2_{g-2}}^{-1}(1-\alpha)$ = 15.5, indicating that both models fit the data well. However, the h value for the log-logistic model is less than that for the logistic model, which indicates that the former model fits the data better than the latter model. Given this, Eq. (3.9) was selected as the final proposed POI model, with β_1 and β_2 equal to -15.36 and 1.06, respectively.

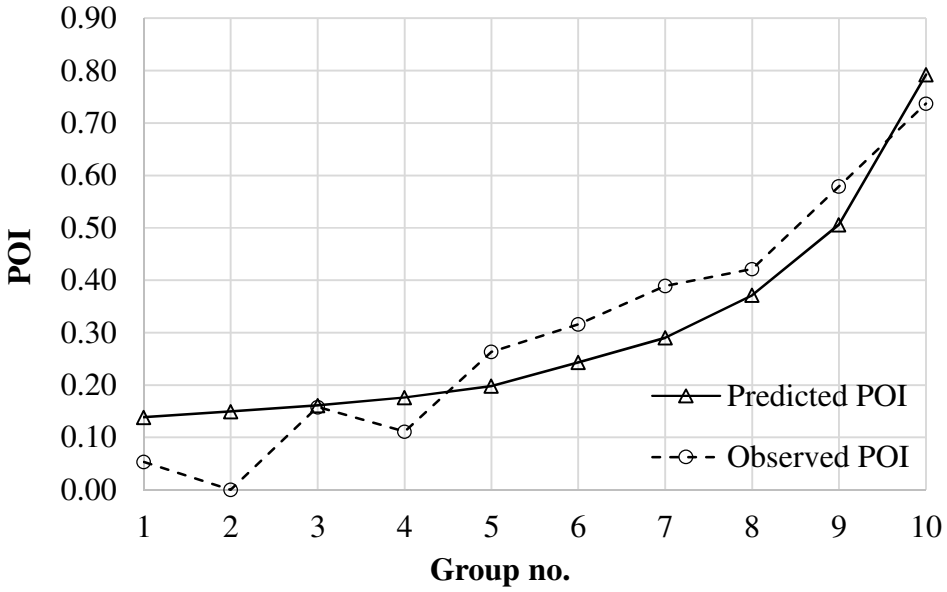

(a)Logistic model

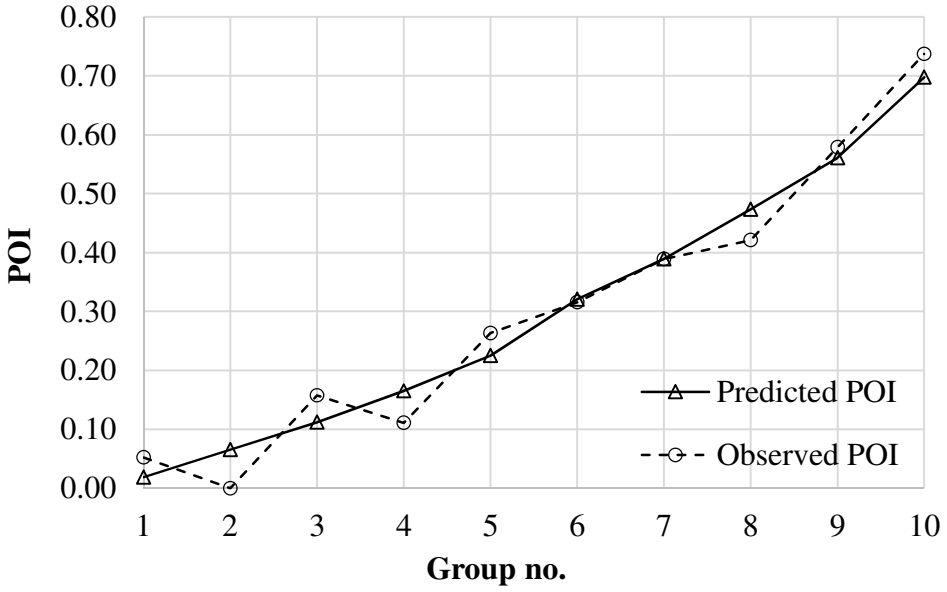

(b) Log-logistic model

Figure 3.2 HL test result for the logistic and log-logistic POI models

To evaluate the confidence interval on the POI value predicted from Eq. (3.9), the so-called logit transformation (Hosmer et al. 2013) was applied to POI such that Eq. (3.9) is rewritten as

$$Y = logit(\mathrm{POI}) = \ln\left(\frac{\mathrm{POI}}{1-\mathrm{POI}}\right) = \beta_1 + \beta_2 \ln(pd^2) \tag{3.11}$$

The confidence interval on Y was then utilized to construct the confidence interval on POI (Hosmer et al. 2013). An estimator of Y, $\hat{Y}$, is given by

$$\hat{Y} = \hat{\beta}_1 + \hat{\beta}_2 \ln(pd^2)$$

and the standard error of $\hat{Y}$, $\mathrm{SE}(\hat{Y})$,is given by (Hosmer et al. 2013)

$$\mathrm{SE}(\hat{Y}) = \left(\left[\mathrm{SE}(\hat{\beta}_1)\right]^2 + 2\ln(pd^2)\,\mathrm{COV}(\hat{\beta}_1, \hat{\beta}_2) + [\ln(pd^2)]^2\left[\mathrm{SE}(\hat{\beta}_2)\right]^2\right)^{\frac{1}{2}} \tag{3.12}$$

where $\mathrm{COV}(\hat{\beta}_1, \hat{\beta}_2)$ is the covariance of $\hat{\beta}_1$ and $\hat{\beta}_2$. An estimator of $\mathrm{SE}(\hat{Y})$, $\widehat{\mathrm{SE}}(\hat{Y})$, can be obtained by substituting the estimators of $\mathrm{SE}(\hat{\beta}_1)$, $\mathrm{SE}(\hat{\beta}_2)$ and $\mathrm{COV}(\hat{\beta}_1, \hat{\beta}_2)$ in Eq. (3.12), all of which are evaluated from the observed Fisher information matrix as described in Section 3.3.2. As $\hat{Y}$ asymptotically follows a normal distribution with the mean equal to the true value of Y and the standard deviation equal to $\mathrm{SE}(\hat{Y})$ (Hosmer et al. 2013), the (1- α)100 percent confidence interval on Y can be estimated as

$$\hat{Y} \pm \Phi^{-1}(1-\frac{\alpha}{2}) \cdot \widehat{\mathrm{SE}}(\hat{Y}) \tag{3.13}$$

where α is usually set to 0.05, which leads to the 95% confidence interval on Y. Finally, the confidence interval on Y is used to evaluate the corresponding confidence interval on POI through Eq. (3.11).

Based on the above-described method, the 95% confidence interval on POI was computed, and the results are depicted in Fig. 3.4. The data points shown in the figure are the same as those shown in Fig. 3.1. The figure shows that almost all the data points are within the 95% confidence interval of the predicted POI, indicating the good

predictive capability of Eq. (3.9). It should be pointed out that the 95% confidence interval is asymmetric with respect to the predicted POI curve. This is because the confidence interval on POI is obtained from the (symmetric) confidence interval on Y through the logit transformation. The 95% upper confidence bound on POI, denoted by POI_{95}, was also evaluated as a conservative estimate of POI and is shown in Fig. 3.3. To facilitate practical application of POI_{95}, the values of POI_{95} corresponding to different values of pd^2 are tabulated in Table 3.4. The tabulation points in the table are plotted on Fig. 3.3, and the values of POI_{95} corresponding to pd^2 values not given in Table 3.4 can be estimated from the linear interpolation.

It is noteworthy that the parameter p in the proposed POI model is the internal pressure at the time of rupture. To predict the probability of ignition for a given pipeline using the proposed model, it is suggested that p be replaced by the normal operating pressure of the pipeline. If a conservative estimate of POI is desirable, p can be set at the maximum allowable operating pressure of the pipeline.

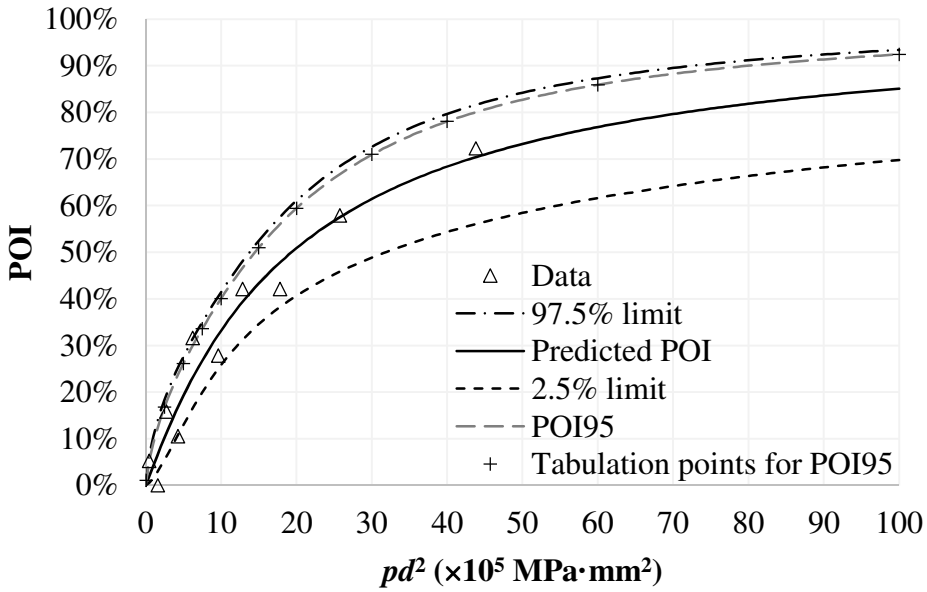

Figure 3.3 Predicted POI with its 95% confidence interval versus pd^2 for the log-logistic POI model

Table 3.4 Look-up table for POI_{95}

pd^2 ($\times 10^5$ MPa-mm^2)	0.05	2.5	5	7.5	10	15	20	30	40	60	100
POI_{95} (%)	1.0	16.7	26.1	33.6	40.0	50.9	59.4	70.9	78.0	85.9	92.4

3.4 Model Validation and Comparison

To validate the proposed log-logistic POI model given by Eq. (3.9), the PIPESAFE rupture incident data (1970-2004) reported by Acton and Baldwin (2008) were employed. Note that the detailed information of individual PIPESAFE data points are confidential and therefore unavailable to the present study. Acton and Baldwin divided the PIPESAFE data into four groups and reported the total number of incidents, mean pd^2 value for the incidents and observed POI value for each of the four groups as summarized in in Table 3.5. The mean pd^2 value for each incident group was then substituted into Eq. (3.9) to evaluate POI and 95% confidence interval on POI using the proposed log-logistic model. The results are shown in Table 3.5. The table shows that the predicted POI values are in reasonable agreement with the observed POI values. The proposed model overestimates POI for the incident group with pd^2 between 10 and 30 ($\times 10^5$ MPa-mm^2) and somewhat underestimates POI for the incident group with pd^2 between 30 and 100 ($\times 10^5$ MPa-mm^2). This could be attributed to two factors: 1) the sample sizes in these two groups are relatively small, and 2) the regional differences between the PIPESAFE data, the majority of which come from European pipeline operators, and the PHMSA data on which the proposed POI model is based.

Table 3.5 PIPESAFE rupture incident data (1970-2004) with corresponding predicted POI values by the proposed POI model

pd^2 Range ($\times 10^5$ MPa-mm^2)	Mean pd^2 for the incidents ($\times 10^5$ MPa-mm^2)	No. of Incidents	Observed POI	Predicted POI	95% confidence Interval
0 to 1	0.4	78	0.05	0.02	(0.01, 0.05)
1 to 10	3.6	77	0.13	0.14	(0.09, 0.21)
10 to 30	17.6	44	0.34	0.47	(0.39, 0.56)
30 to 100	48.2	29	0.83	0.72	(0.60, 0.82)

The proposed log-logistic POI model is compared with the simple linear regression POI model given by Eq. (3.1) in Fig. 3.5. The "PIPESAFE 70-96", "PIPESAFE 70-04" and "PIPESAFE 70-04 + PHMSA 02-07" curves in the figure represent the linear regression POI models fitted using different sets of pipeline rupture incident data as described in Section 3.1. The figure shows that unlike the bilinear characteristic of the linear regression POI models the log-logistic POI model is characterized by a single smooth curve and naturally bounded by zero and unity. Furthermore, the POI values obtained from the log-logistic model are higher than those from the linear regression models for pd^2 values between 3 and 40 ($\times 10^5$ MPa-mm^2) and somewhat lower than those from the linear regression models for pd^2 values between 40 and 70 ($\times 10^5$ MPa-mm^2). For pd^2 values between 70 and 100 ($\times 10^5$ MPa-mm^2), the POI values obtained from the log-logistic model are close to the upper bound of the linear regression models.

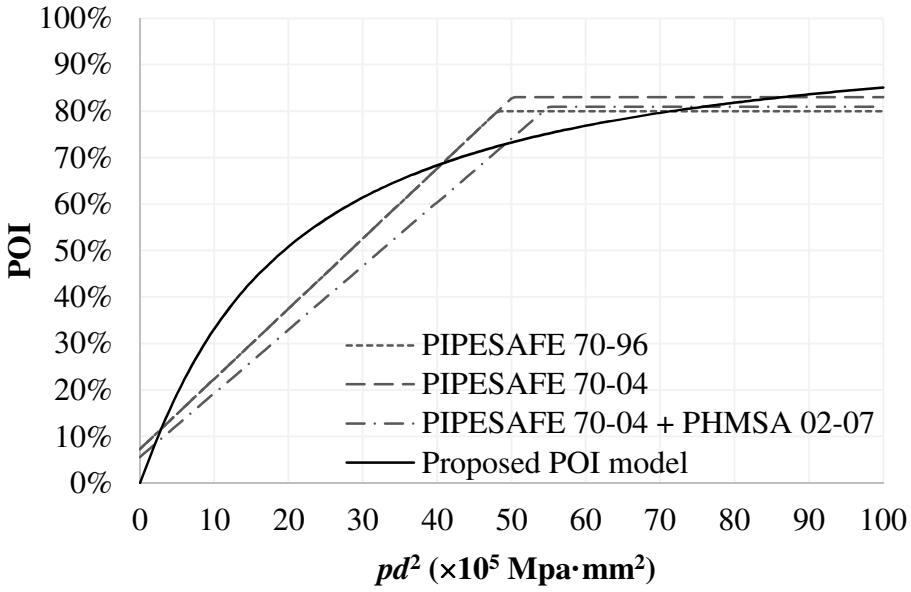

Figure 3.4 Proposed POI model compared with simple linear regression POI model

3.5 Conclusions

A total of 188 rupture incidents that occurred on onshore natural gas transmission pipelines in the US between 2002 and 2014 were identified from the PHMSA pipeline incident database to develop a POI model given rupture of gas pipelines. Fifty-nine of those incidents involved ignition. Both the logistic and log-logistic functions were considered for the POI model. The predictors considered in the model include the location class of the pipeline and product of the internal pressure at the time of incident and outside diameter of the pipeline squared, i.e. pd^2, which is directly related to the initial gas outflow after a rupture. The maximum likelihood method was employed to evaluate the parameters of the POI models. It was observed that pd^2 is strongly correlated with POI, whereas the location class is not strongly correlated with POI. The Hosmer-Lemeshow test suggests that the log-logistic POI model fits the PHMSA incident data better than the logistic POI model; therefore, the log-logistic POI model with pd^2 as the sole predictor was selected as the proposed POI model.

The 95% confidence interval and 95% upper confidence bound on the predicted POI were evaluated. To facilitate practical application, the values of the 95% upper

confidence bound on POI corresponding to different values of pd^2 were tabulated in a look-up table. To validate the proposed POI model, the POI values predicted by the model were compared with the observed POI values for four groups of PIPESAFE rupture incidents reported in the open literature. The comparison indicates that the predicted and observed POI values are in reasonable agreement; the discrepancy may be attributed to the regional differences between the PIPESAFE incidents (mostly in Europe) and PHMSA incidents.

The proposed POI model is more advantageous than the simple linear regression-based POI model reported in the literature in that the former is naturally bounded by zero and unity, and associated with desirable statistical properties such as the confidence interval and upper confidence bound. To apply the proposed POI model in the quantitative risk assessment of a given pipeline, it is suggested that the internal pressure at the time of the incident be replaced by the normal operating pressure, or by the maximum allowable operating pressure if a conservative estimate of POI is preferred.

References

Acton, M.R., Baldwin, T.R. and Jager, E.E. 2002. Recent developments in the design and application of the PIPESAFE risk assessment package for gas transmission pipelines. In 2002 4th International Pipeline Conference. American Society of Mechanical Engineers, pp. 831-839.

Acton, M.R. and Baldwin, P.J. 2008. Ignition probability for high pressure gas transmission pipelines. In 2008 7th International Pipeline Conference. American Society of Mechanical Engineers, pp. 331-339.

ASME 2013. ASME B31.8: Gas transmission and distribution piping systems. The American Society of Mechanical Engineers, Three Park Avenue, New York, NY.

Hosmer Jr, D.W., Lemeshow, S. and Sturdivant, R.X. 2013. Applied logistic regression, 3rd edition. John Wiley & Sons, Inc., Hoboken, New Jersey.

Leemans, D.V. and Frosyth, D. 2004. Bayesian approaches to using field test data in determining the probability of detection. Materials Evaluation, 62(8): 855-859.

Lu, D., Skow, J. and Keane, S. 2014. Assessing the Probability of Detecting Crack Features Using Ultrasonic In-Line Inspection Tool Run Results and Excavation Data. In 2014 10th International Pipeline Conference. American Society of Mechanical Engineers, Paper No. IPC2014-33248.

Maindonald, J.H. 2008. Using R Data Analysis and Graphics: Introduction, Code and Commentary. Australian National University. Centre for Mathematics and Its Applications.

Nessim, M.A., Zhou, W., Zhou, J. and Rothwell, B. 2009. Target reliability levels for design and assessment of onshore natural gas pipelines. Journal of Pressure Vessel Technology, ASME, 131(6), 061701.

NTSB. 2003. Natural gas pipeline rupture and fire near Carlsbad, New Mexico, August 19, 2000. Pipeline Accident Report NTSB/PAR-03/01, National Transportation Safety Board, Washington, D.C.

NTSB. 2011. Pacific Gas and Electric Company natural gas transmission pipeline rupture and fire, San Bruno, California, September 9, 2010. Pipeline Accident Report NTSB/PAR-11/01, National Transportation Safety Board, Washington, D.C.

Siedlecki, R. 2011. Method of determining warning signals based on a company's financial cycle of live using logistic and log-logistic function. Economics, Management, and Financial Markets,(1): 1030-1038.Carroll, R.J. and Ruppert, D. 1988. Transformation and weighting in regression. CRC Press.

USOFR (US Office of the Federal Register). 2013. Code of Federal Regulations (CFR). 2013. Title 49: Transportation, parts 178 to 199, US Government Printing Office, Washington, DC 20402.

Zheng, R., and Ellingwood, B.R. 1998. Role of non-destructive evaluation in time-dependent reliability analysis. Structural Safety, 20(4): 325-339.

Chapter 4

Quantitative Risk Assessment of a Hypothetical Onshore Natural Gas Transmission Pipeline

4.1 Introduction

Quantitative risk assessments of oil and gas pipelines are becoming more and more accepted by pipeline operators as an integral component of the pipeline integrity management program. The risks posed by natural gas pipelines are mostly related to the human safety. Two well-known quantitative risk measures in terms of the human safety are the societal and individual risks (TNO Purple Book 1999; Tomic et al. 2014). The societal risk associated with a given pipeline characterizes the aggregate risk over a group of people living near the pipeline, whereas the individual risk associated with the pipeline characterizes the risk the pipeline poses to a given individual who happens to be in its vicinity.

The objective of the study reported in this chapter is to conduct the quantitative risk assessment of a hypothetical onshore natural gas pipeline, by employing the pipeline failure statistics reported in Chapter 2 and the probability of ignition (POI) model proposed in Chapter 3.

The rest of the chapter is organized as follows. Section 4.2 describes the methodologies for evaluating the societal and individual risk levels associated with natural gas pipelines. The risk assessment of a hypothetical gas pipeline is described in Section 4.3, followed by summary and conclusions in Section 4.4.

4.2 Methodologies for Risk Assessments

4.2.1 Thermal Radiation Effect of an Ignited Rupture

As discussed in Chapter 3, there are typically three failure modes associated with an onshore gas pipeline: leak, puncture and full-bore rupture. A non-ignited failure of a gas pipeline has a negligible impact on the safety of the population in the vicinity of the

pipeline. On the other hand, the human safety-related consequences associated with ignited ruptures can be very severe and typically much greater than those associated with ignited leaks and punctures. Therefore, the risk assessments presented in this chapter are with respect to ignited ruptures. An ignited rupture of a gas pipeline emits thermal radiation to the area surrounding the rupture site, which may cause burn injuries and fatalities depending on the thermal load received by the population within the area. The thermal load is a function of the exposure time and thermal radiation intensity (Lees 1996). Given an ignited rupture, it is involved to carry out detailed evaluations of the thermal load received by each individual impacted by the rupture as the evaluation needs to take account of the distance between the individual and rupture site, shape, nature and extent of the fire, the atmospheric transmissivity between the fire and the individual as determined by the humidity, escape speed of the individual, and availability of shelters in the immediate vicinity of the individual (Acton et al. 2002). In this study, a widely accepted simplified model, namely the C-FER model (Stephens 2002), was adopted to evaluate the thermal radiation hazard zone associated with an ignited rupture. The C-FER model assumes a double-ended gas release for a rupture with the diameter of the release hole at each end equal to the pipe diameter. The radius of the circular thermal radiation hazard area, r_h (m), within which the heat intensity level exceeds a certain threshold, I_{th} (kW/m^2), is given by

$$r_h = \sqrt{\frac{0.1547pd^2}{I_{th}}} \tag{4.1}$$

where p (MPa) is the pipeline pressure at the time of rupture and d (mm) is the pipeline outside diameter. Therefore, the radius of the thermal radiation hazard zone due to an ignited rupture incident can be determined from the pressure, diameter and thermal radiation intensity threshold using the C-FER model.

By assuming a typical exposure time of 30 s (Rothwell and Stephens 2006), the values of I_{th} corresponding to the onset of burn injury, 0% lethality and 100% lethality for people under outdoor exposure were chosen to be 5.05, 12.62 and 31.55 kW/m^2, respectively, based on previous studies reported in the literature (Eisenberg et al. 1975; Hymes 1983;

Bilo and Kinsman 1997). The lethality associated with a given location that is within the annulus bounded by the 0% and 100% lethality is obtained from linear interpolation for simplicity.

For the indoor exposure condition, wooden structures are unlikely to ignite with a thermal radiation intensity lower than 15.77 kW/m^2, and hence should afford indefinite protection to occupants (Bilo & Kinsman 1997; Stephens 2002). If the thermal radiation intensity is greater than 31.55 kW/m^2, such structures will ignite fast (not more than 65 seconds) and provide no protection after ignition (Bilo and Kinsman 1997; Stephens 2002). The values of I_{th} corresponding to 0% and 100% probabilities of ignition of a wooden structure were therefore chosen to be 15.77 and 31.55 kW/m^2, respectively. The probability of ignition of a wooden structure associated with a given location that is within the annulus bounded by the 0% and 100% probabilities is obtained from linear interpolation for simplicity. Given ignition of a wooden structure, people inside the structure were assumed to be able to escape outdoors and then subjected to the outdoor exposure; therefore, the values of I_{th}, corresponding to the outdoor exposure condition are applicable. The selected values of I_{th} and corresponding implications for the human safety for the outdoor and indoor exposure conditions are summarized in Figs. 4.1(a) and 4.1(b), respectively. Note that $r_{12.62}$, $r_{15.77}$ and $r_{31.55}$ in these figures denote the radii of the circular thermal radiation hazard areas corresponding to the heat intensity levels of 12.62, 15.77 and 31.55 kW/m^2, respectively.

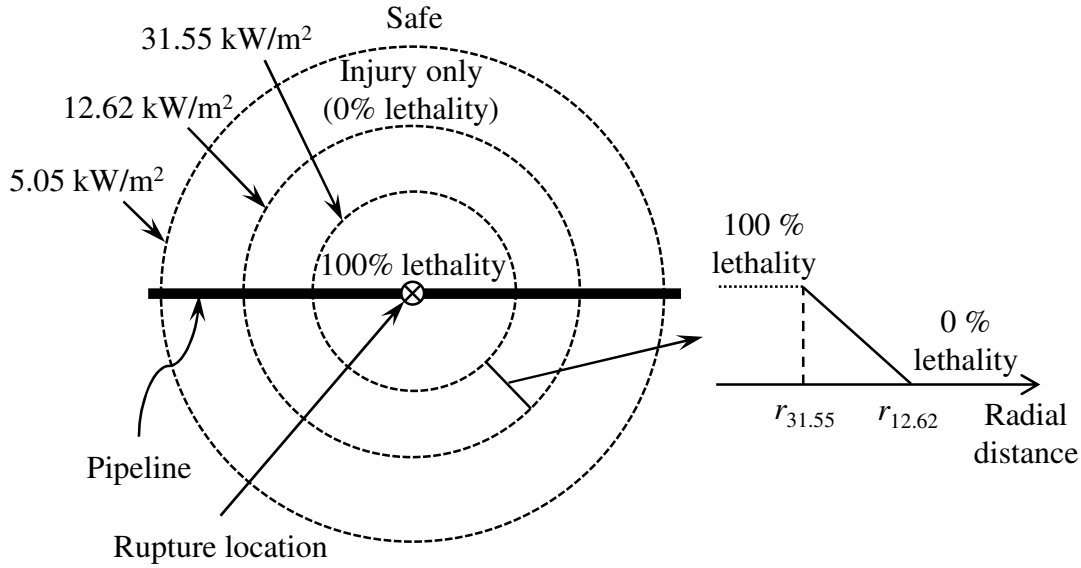

(a) Outdoor exposure

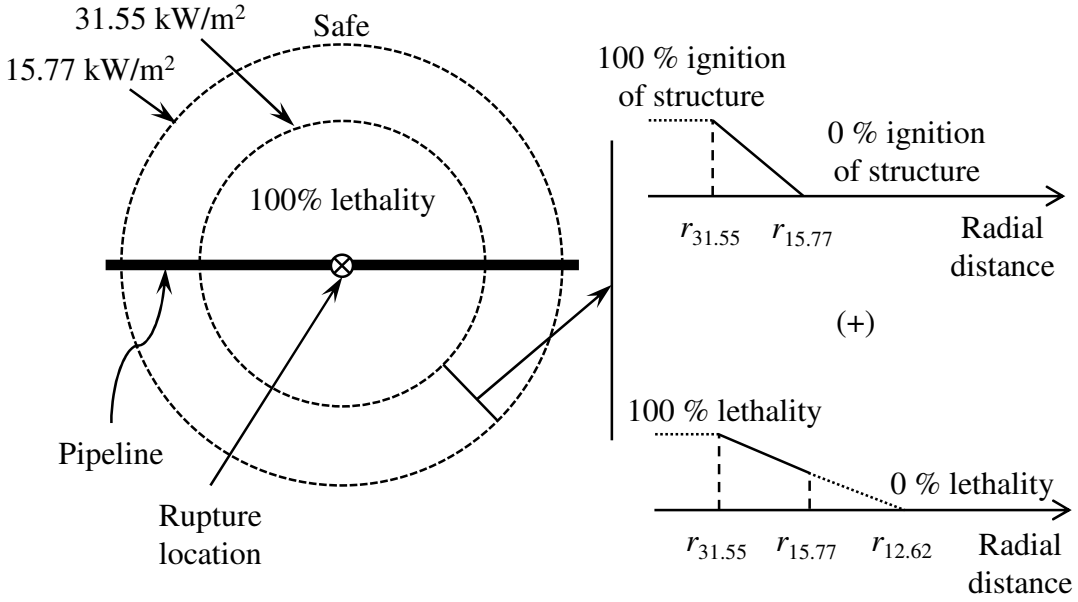

(b) Indoor exposure

Figure 4.1 Thermal radiation intensity thresholds and human safety implications

4.2.2 Societal Risk

The societal risk can be represented by the expected number of casualties per km-year (Nessim et al. 2009) and the so-called F-N curve (TNO Purple Book 1999). Note that the F-N curve is defined as the frequency (i.e. F) of incidents causing N (N = 1, 2, ...) or more casualties, and typically plotted on a log-log scale with the vertical and horizontal axes representing F and N, respectively.

The societal risk in terms of the expected number of casualties per km-year associated with a given location, x, on a gas pipeline can be calculated as follows:

$$R_s(x) = F_r(x) \cdot \text{POI} \cdot C_s(x) \tag{4.2}$$

where $F_r(x)$ is the probability of rupture of the pipeline at location x (per km-year), POI is the probability of ignition given rupture, and $C_s(x)$ is the weighted average number of casualties caused by an ignited rupture at x. Note that $F_r(x)$ can be evaluated from structural reliability analyses if probabilistic information about the pipeline and threats are available. Otherwise, historical pipeline failure statistics such as those reported in Chapter 2 can be used to estimate $F_r(x)$. The value of POI can be obtained from the log-logistic POI model (Eq. 3.9) developed in Chapter 3.

To plot the F-N curve for a given one-kilometer long segment of the pipeline, the pipeline segment is first divided into n equal-length sections. The probability of ignited rupture per year, $f(j)$, of the j^{th} (j=1, 2, …, n) section is then calculated as follows:

$$f(j) = f_r(j) \cdot \text{POI} \tag{4.3}$$

where $f_r(j)$ is the annual probability of rupture of the j^{th} section. The frequency of ignited ruptures causing N (N = 1, 2, ...) or more casualties, $F(N)$, for the one-kilometer pipeline segment is given by

$$F(N) = \sum_{N(j) \geq N} f(j) \;\; (j = 1, 2, \dots, n;\; N = 1, 2, \dots) \tag{4.4}$$

where $N(j)$ is the number of casualties caused by the ignited rupture of the j^{th} section. In estimating $N(j)$, the rupture site is assumed to be at the mid-point of the j^{th} section. It should be noted that given the rarity of pipeline incidents, the frequency of rupture per km-year is equivalent to the probability of rupture per km-year.

4.2.3 Individual Risk

Different from the evaluation of the societal risk, the individual risk is quantified as the annual probability of casualty (i.e. fatality or injury) imposed on an individual located near the pipeline by the pipeline interaction length, l, as shown in Fig. 4.2. An ignited rupture of the pipeline within the interaction length will affect the individual. The interaction length l can be calculated as $2(r_{max}^2 - y^2)^{0.5}$ for $y \leq r_{max}$, where $r_{\max}$ (m) is the maximum impact radius given an ignited rupture and y (m) is the offset distance of the individual from the pipeline. In this study, the maximum impact radii given an ignited rupture are the radii of the circular thermal radiation hazard areas corresponding to the heat intensity levels 5.05 and 15.77 kW/m^2, respectively, for outdoor and indoor individuals. The risk for an individual near the pipeline can be calculated as follows.

$$R_i(y) = \int_0^l F_r(z) \cdot \text{POI} \cdot C_i(z, y) dz, \text{ for } y \leq r_{max}; \tag{4.5a}$$

$$R_i(y) = 0, \text{ for } y > r_{max}. \tag{4.5b}$$

where $F_r(z)$ is the probability of rupture of the pipeline at location z (per km-year), and $C_i(z, y)$ is the probability of burn jury and lethality to the individual having an offset distance y from the pipeline caused by an ignited rupture at z ($0 \leq z \leq l$) within the pipeline interaction length. Given the values of z and y (see Fig. 4.2), the distance between the individual and the rupture location z can be calculated as $[(l/2 - z)^2 + y^2]^{0.5}$ and then $C_i(z, y)$ can be determined using Figs. 4.1(a) and 4.1(b), respectively, for the outdoor and indoor exposure conditions. In this study, the individual risk was computed numerically by assigning a unit length (1 m) to dz.

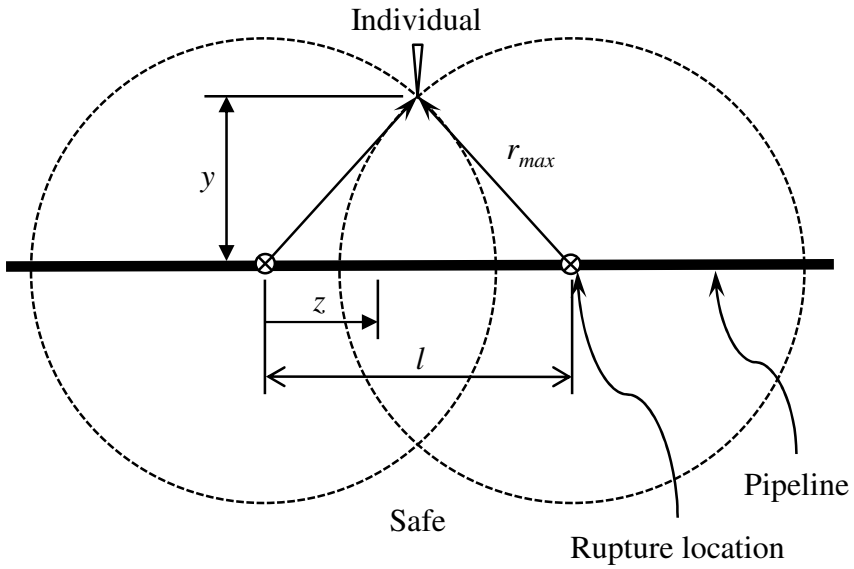

Figure 4.2 Interaction length for individual risk with offset distance *y*

4.3 Hypothetical Example

4.3.1 General

A hypothetical natural gas transmission pipeline is employed to illustrate the quantitative risk assessment procedure described in Section 4.2. The pipeline has a nominal pipe diameter (NPS) of 24 inches (609.6 mm), and an operating pressure of 6.0 MPa. Approximately 2.3 km of the pipeline traverses a residential area that consists of many single-family houses (SglFamily), one meeting and recreation facility (MtgRecF), one school and several playgrounds (PlayGrnd). The route of the pipeline and its surrounding buildings in the residential area are shown in Fig. 4.3.

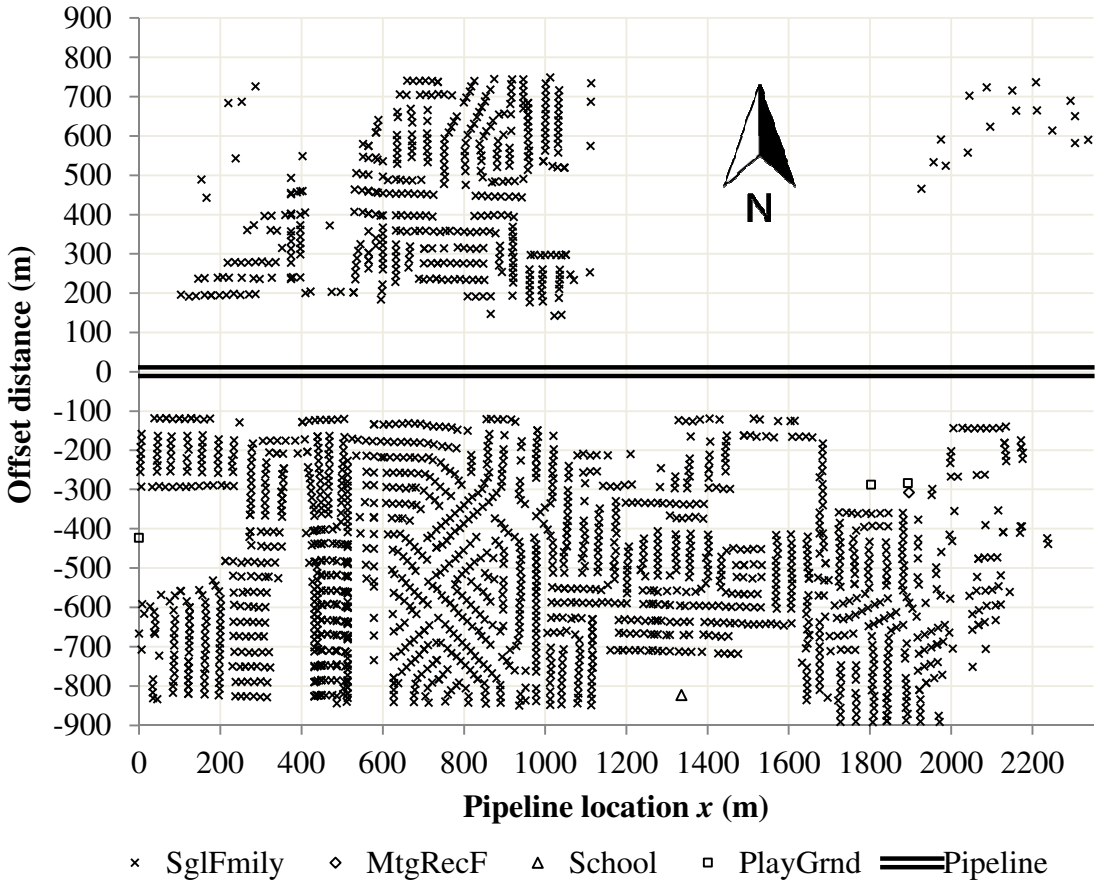

Figure 4.3 Illustration of a hypothetical pipeline and its sourroudings

The historical pipeline failure statistics obtained from the PHMSA incident database as reported in Chapter 2 were used to evaluate the probability of rupture of the example pipeline. The 12-year average rupture rate of pipelines with diameter $20 < d \leq 28$ inches due to all failure causes combined was estimated to be 2.5×10^{-5} per km-year in Chapter 2. This value was selected as the representative rupture rate for the example pipeline. The value of POI given rupture for the example pipeline was evaluated to be 0.53 by substituting the operating pressure of 6.0 MPa and diameter of 609.6 mm into Eq. (3.9). The radii of the circular thermal radiation hazard areas in Fig. 4.1 corresponding to the threshold heat intensity levels 31.55, 15.77, 12.62 and 5.05 kW/m^2 are equal to 105, 148, 165 and 261 m, respectively.

To evaluate the societal risk posed by the example pipeline, the number of occupants in each of the four different types of facilities (i.e. single-family house, meeting and recreating facility, school and playground) indicated in Fig. 4.3 needs to be estimated. The average number of people living in a single-family house was assumed to be 2.9 based on the 2011 Census Report of Statistics Canada (Milan & Bohnert 2012). It is further assumed that the occupants are present in the house on average 50% of the time. It follows that the expected number of occupants in the house at the time of the pipeline rupture equals 1.5. The average number of people occupying the meeting and recreation facility was arbitrarily assumed to be 100, and the facility was assumed to open eight hours a day and seven days a week. Therefore, the expected number of occupants in the facility at the time of rupture equals $100 \times 8/24 = 33.3$. The average number of people in the school was assumed to be 400 based on the information provided by the Council of Ministers of Education, Canada (accessed from http://www.cmec.ca/299/Education-in-Canada-An-Overview/ on 20th January, 2015), and the school was assumed to be open eight hours a day and five days a week. Therefore, the expected number of occupants at the time of rupture equals $400 \times 8/24 \times 5/7 = 95.2$. The playground was assumed to be on average occupied by 20 people for eight hours a day; therefore, the expected number of occupants at the time of rupture equals $20 \times 8/24 = 6.7$. Finally, it was assumed that the people in the playground at the time of rupture are subjected to the outdoor exposure, while those in the single-family house, meeting and recreation facility and school are subjected to the indoor exposure. A summary of the above assumptions for different facilities is shown in Table 4.1.

Table 4.1 Summary of assumptions for different facilities

Type of facility	Number of occupants	Expected number of occupants at the time of rupture	Exposure type
SglFamily	2.9	1.5	Indoor
MtgRecF	100	33.3	Indoor
School	400	95.2	Indoor
Playgrnd	20	6.7	Outdoor

To evaluate the individual risk, it is conservatively assumed that an individual is present in the invicinity of the pipeline 100% of the time. The individual risk levles corresponding to both the outdoor and indoor exposures were evaluated.

4.3.2 Results of Risk Analyses

The quantified societal risk in terms of the expected number of casualties is shown in Fig. 4.4. The figure shows that that the societal risk level in terms of the expected number of fatalities are the lowest at x approximately equal to 1200 and 1800 m, and relatively high at x of around 500, 900 and 1400 m. This can be explained by the distribution of buildings around the pipeline. In Fig. 4.3, at x around 1200 and 1800 m, nearby buildings are located relatively farther (> 200 m) from the pipeline compared to other portions of the pipeline. For x around 500, 900 and 1400 m, the closest buildings are only about 100 m away from the pipeline, and thus the societal risk levels in terms of the expected number of fatalities in the locations are relatively high. The variation of the societal risk level in terms of the expected number of casualties (i.e. fatalities plus injuries) along the pipeline location is similar to that of the societal risk level in terms of the expected number of fatalities. The highest societal risk level in terms of the expected number of fatalities is estimated to be 4.9×10^{-5} per km-year, while the highest societal risk level in terms of the expected number of casualties is estimated to be 7.8×10^{-5} per km-year.

From Figs. 4.3 and 4.4, it can be inferred that the societal risk level is largely influenced by the relative locations between the pipeline and its surrounding buildings. If the offset distances of the buildings south of the pipeline are increased by just 5 m, the estimated highest societal risk level in terms of the expected number of fatalities can be lowered to 3.3×10^{-5} per km-year, a 33% reduction of the risk level.

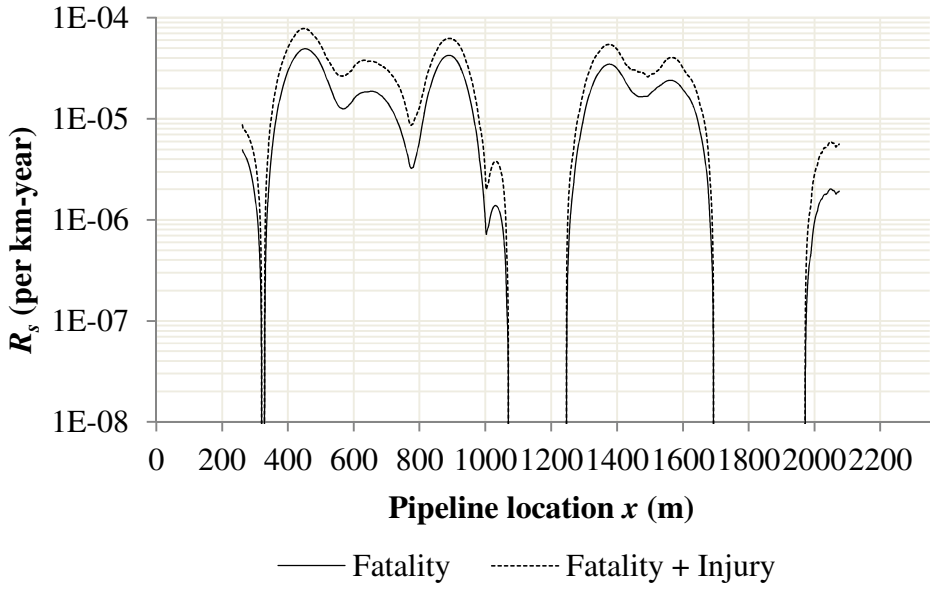

Figure 4.4 Societal risk level in terms of the expected number of casualites

The quantified societal risk level in terms of the F-N curve per km is plotted in Fig. 4.5. Note that the F-N curve per km in this example was evaluated as follows: the F-N curve for the first one-km pipeline segment that starts at $x = 0.261$ km was evaluated; then the F-N curve for the next one-km segment that starts at $x = 0.461$ km was evaluated, and so on. Only the F-N curve in terms of fatality was investigated and a total of five F-N curves were computed as a result. Figure 4.5 shows that the F-N curves intercept each other and as a result it is not possible to identify a single most critical F-N curve over the entire range of N. However, the F-N curve corresponding to the first one-km segment envelopes the other F-N curves for $N \geq 2$.

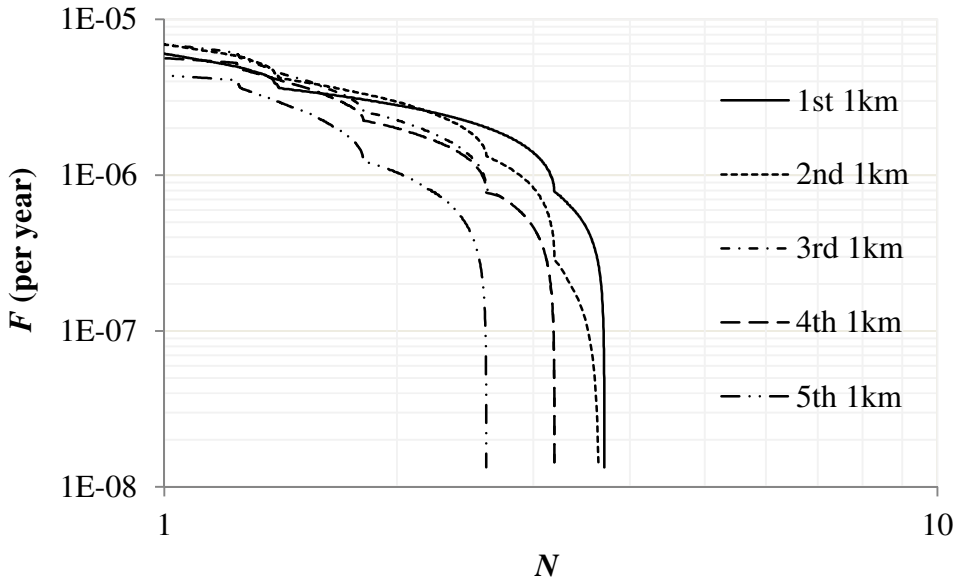

Figure 4.5 Societal risk level in terms of *F-N* curve

The quantified individual risks for the outdoor and indoor exposures are shown in Fig. 4.6. The indivdual risk is a function of the offset distance, *y*, of the individual from the pipeline. The figures show that the offset distance beyond which the individual risk becomes zero equals 261 and 148 m, for the outdoor and indoor exposures, respectively. The highest individual fatality risks equal 3.6×10^{-6} and 3.2×10^{-6} per year, respectively, for the outdoor and indoor exposures, and the hightest individual casualty risks equal 7.0×10^{-6} and 3.4×10^{-6} per year, for the outdoor and indoor exposures, respectively.

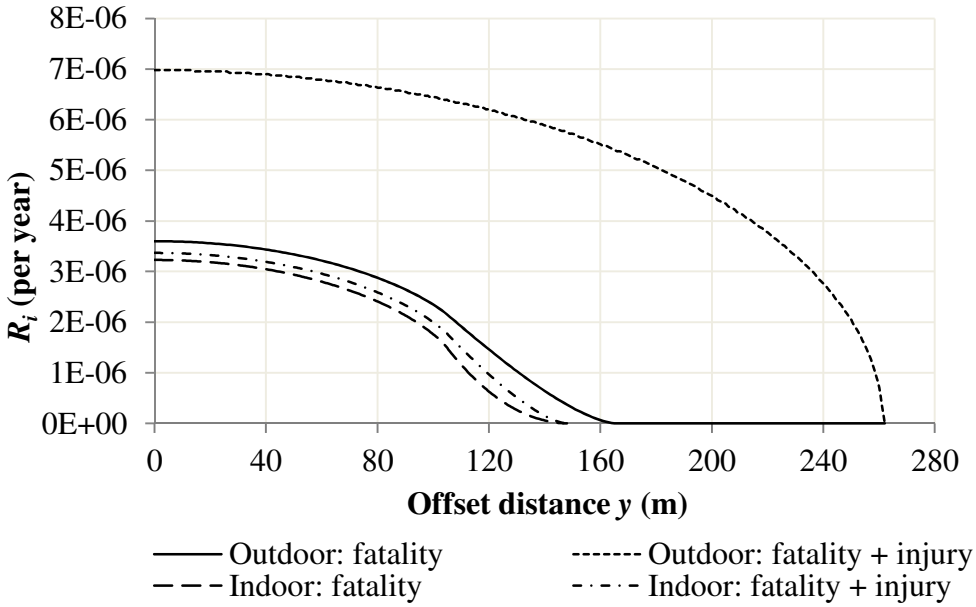

Figure 4.6 Individual risk levels for outdoor and indoor exposures

4.4 Conclusions

The methodologies for quantifying the risks in terms of the human safety due to ignited ruptures of onshore gas transmission pipelines are discussed in this chapter. The well-known C-FER model was adopted to evaluate the radii of the thermal radiation hazard areas resulting from ignited ruptures of onshore gas pipelines. According to this model, the radius of the thermal radiation hazard area can be evaluated from the pressure and diameter of the pipeline, and the heat intensity threshold corresponding to a given degree of burn injury to humans. Based on the literature review, the heat intensity thresholds corresponding to the onset of burn injury, 0% lethality and 100% lethality were selected to 5.05, 12.62 and 31.55 kW/m^2, respectively, for the outdoor exposure condition. For the indoor exposure condition, the heat intensity thresholds corresponding to 0% and 100% probabilities of ignition of a wooden structure were selected to be 15.77 and 31.55 kW/m^2, respectively. It is assumed that a wooden structure is able to afford indefinite protection to its occupants for heat intensity levels less than 15.77 kW/m^2. Given ignition of a wooden structure, its occupants were further assumed to escape outdoors and subject to outdoor exposure.

Both the societal and individual risks are considered. The societal risk is represented by the expected number of casualties per km-year as well as the F-N curve for any one-km segment of the pipeline. The individual risk is represented by the annual probability of casualty for an individual in the vicinity of the pipeline. Quantitative risk assessments of a hypothetical onshore gas transmission pipeline were carried out to illustrate the methodologies. The pipeline was assumed to have an outside diameter of 609.6 mm and operating pressure of 6.0 MPa, and cross a residential area that is approximately 2.3 km long. The probability of rupture per km-year of the pipeline was estimated based on the historic failure statistics summarized in Chapter 2, whereas POI given rupture of the pipeline was evaluated from the log-logistic POI model proposed in Chapter 3. The analysis results indicate that the societal risk in terms of the expected number of casualties and F-N curve varies along the pipeline, due to the different locations and types of the buildings or facilities intended for human occupants along the pipeline. For this particular example, a slight increase in the offset distance by 5 m resulted in a 33% reduction in the maximum societal risk in terms of the expected number of fatalities. The individual risk is a function of the indoor and outdoor exposure condition as well as the offset distance of the individual with respect to the pipeline.

References

Acton, M.R., Baldwin, T.R. and Jager, E.E. 2002. Recent developments in the design and application of the PIPESAFE risk assessment package for gas transmission pipelines. In 2002 4th International Pipeline Conference. American Society of Mechanical Engineers, pp. 831-839.

Bilo, M., and Kinsman, P. 1997. Thermal radiation criteria used in pipeline risk assessment. Pipes & Pipelines International, 42(6): 17-25.

Eisenberg, N.A., Lynch, C.J., and Breeding, R.J. 1975. Vulnerability Model: A Simulation System for Assessing Damage Resulting from Marine Spills. Environmental Control, Report CG-D-136-75, Rockville, MD, USA.

Hymes, I. 1983. The physiological and pathological effects of thermal radiation. Safety and Reliability Directorate, Report SRD, R275, Culcheth, Warrington, UK.

Lees, F.P. 1996. Loss prevention in the process industries: Hazard identification, assessment and control. Butterworth-Heinemann, Oxford, UK.

Milan, A. and Bohnert, N. 2012. Fifty years of families in Canada: 1961 to 2011. 98-312-X2011003, Minister of Industry, Ottawa.

Nessim, M., Zhou, W., Zhou, J., and Rothwell, B. 2009. Target reliability levels for design and assessment of onshore natural gas pipelines. Journal of Pressure Vessel Technology, 131(6): 061701.

Rothwell, B. and Stephens, M. 2006. Risk analysis of sweet natural gas pipelines: Benchmarking simple consequence models. In 2006 International Pipeline Conference. American Society of Mechanical Engineers, pp. 911-919.

Stephens, M.J., Leewis, K. and Moore, D.K. 2002. A model for sizing high consequence areas associated with natural gas pipelines. In 2002 4th International Pipeline Conference. American Society of Mechanical Engineers, pp. 759-767.

TNO Purple Book. (1999). Guideline for quantitative risk assessment. The Netherlands: Committee for the Prevention of Disasters.

Tomic, A., Kariyawasam, S. and Kwong, P. 2014. Effective Consequence Evaluation for System Wide Risk Assessment of Natural Gas Pipelines. In 2014 10th International Pipeline Conference. American Society of Mechanical Engineers, pp. V003T12A019-V003T12A019.

Zhou, W., and Nessim, M.A. 2011. Optimal design of onshore natural gas pipelines. Journal of Pressure Vessel Technology, 133(3): 031702.

Chapter 5 Summary and Conclusions

5.1 Statistical Analyses of PHMSA data

To provide insights into the current state of gas transmission pipelines in the US and derive relevant failure statistics as the baseline failure probabilities for carrying out system-wide risk assessments of pipelines, statistical analyses of incidents on onshore gas transmission pipelines were carried out based on the PHMSA database. The mileage and pipe-related incident data corresponding to onshore gas transmission pipelines in the US between 2002 and 2013 were investigated. The format of the incident data of 2002-2009 is different from that of the incident data of 2010-2013; therefore, the two sets of data were aggregated according to sets of failure causes or failure modes adopted in this study. The adopted failure causes include the internal and external corrosions (IC and EC), third-party excavation (TPE), material failure (MF), first- and second-party excavation (FSPE), previously damage pipe (PDP), vehicle not engaged in excavation (V) and others (O). The failure modes were categorized as leak, puncture, and rupture and other.

The total lengths of the onshore gas transmission pipelines in the US from 2002 to 2003 varied between 470,000 and 480,000 km, and the total length remained around 480,000 km since 2009. Newer pipelines gradually replaced older pipelines with time as expected, however, approximately 60% of the pipelines were more than 45 years old as of 2013. About 80% of pipelines are in Class 1 areas, whereas about 20% of pipelines are in Class 2 and Class 3 areas with less than 1% of pipelines being in Class 4 areas. Almost all pipelines are steel pipelines, about 98% of which are cathodically protected and coated (CC).

The analyses of the pipeline incident data identified the third party excavation (26.3%), external corrosion (23.7%), material failure (16.8%) and internal corrosion (8.4%) as the main failure causes. TPE- or IC-caused incidents occurred mostly on pipelines with small or medium diameters (i.e. $4 < d \leq 20$ inches), whereas EC- or MF-caused incidents occurred mostly on pipelines with medium or large diameters (i.e. $d > 10$ inches). The pipes or field-welding or both in the 1950s may be of relatively poor quality given the

fact that the percentage of the MF-caused incidents having occurred on pipelines installed in the 1950s were disproportionately higher than the contribution of such pipelines to the total mileage. A significant portion of the TPE-caused incidents occurred on Class 3 pipelines. Rupture is the most common failure mode with 38% of the incidents resulting in ruptures, while 30 and 20% of the incidents resulted in leak and puncture, respectively. The average probability of ignition given a rupture, leak or puncture equals 30, 3 or 10%, respectively. Seventy-five and eighty-three percents, respectively, of a total of 16 fatalities and 75 injuries resulting from the 464 pipe-related incidents between 2002 and 2013 were caused by rupture incidents.

The analyses of rupture incident rates (per km-year) were conducted using the mileage and incident data for onshore gas transmission pipelines. The 12-year average rupture rate equals 3.1×10^{-5} per km-year due to all failure causes combined. EC is the leading cause for rupture of all pipelines installed in the 1960s or earlier. The three-year moving average rupture rate due to TPE gradually decreased since 2007 and that due to EC and MF, respectively, decreased and increased since 2009. The TPE-caused rupture rate is markedly higher on Class 3 pipelines than on Class 1 and Class 2 pipelines, suggesting the safety factor adopted in the design code for Class 3 pipelines may be inadequate in terms of preventing the third-party excavation damage.

5.2 Probability of Ignition Model Development

The logistic and log-logistic functions with two predictors, which are the location class of the pipeline and the product of the internal pressure at the time of incident and outside diameter of the pipeline squared (pd^2), were considered as the candidate probability of ignition (POI) models for ruptures of onshore gas transmission pipelines. A total of 188 rupture incidents, 59 out of them being ignited incidents, of onshore gas transmission pipelines in the US between 2002 and 2004 were collected from the PHMSA pipeline incident database to develop the POI models. The model parameters were estimated using the maximum likelihood method, and the pd^2 was found to be strongly correlated with POI but the location class was not. According to the Hosmer-Lemeshow test, the log-logistic POI model was found to be better than the logistic POI model in terms of

fitting the data set. Therefore the former model was selected as the final proposed POI model with pd^2 as the sole predictor in the model.

The 95% confidence interval and 95% upper confidence bound for the proposed POI model were evaluated and the latter was tabulated in a look-up table to facilitate the practical application of the proposed POI model. A set of observed POI values for four groups of PIPESAFE rupture incidents reported in the open literature was used to validate the proposed POI model. The results show that the model predictions agree reasonably well with the observed POI values, and the regional differences between the PIPESAFE incidents (mostly in Europe) and PHMSA incidents may give rise to the discrepancy between them.

The proposed POI model overcomes the drawbacks associated with the simple linear regression-based POI model reported in the literature in that it has natural probability properties and statistics such as the confidence interval and upper confidence bound for practical application.

5.3 Quantitative Risk Assessment of Onshore Gas Pipelines

The rupture incident rates obtained in Chapter 2 and the log-logistic POI model proposed in Chapter 3 were incorporated in the practical application of the quantitative risk assessment for a hypothetical onshore gas transmission pipeline presented in Chapter 4. The quantitative risk assessment considered the societal and individual risks posed by the pipeline on the population located in the vicinity of the pipeline. The societal risk was evaluated in terms of the expected number of casualties and *F-N* curve, while the individual risk was evaluated as the annual probability of casualty for a given individual located near the pipeline. The size of the thermal radiation hazard zone given an ignited rupture for the outdoor and indoor exposure conditions was evaluated using the well-known CFER model and selected thermal radiation thresholds corresponding to different levels of burn injury. Based on the rupture incident rates, log-logistic POI model and thermal radiation hazard model, the societal and individual risks were computed. In the

calculation of the societal risk, the average number of occupants and likelihood of presence of the occupants for the single family house, meeting and recreation facility, school and playground were assumed based on the information in the literature.

The societal risk was observed to be related with the relative locations between the pipeline and its surrounding buildings. The individual risk is a function of the offset distance between the individual and the pipeline, and the risk decreases as the offset distance increases.

5.4 Recommendations for future study

Recommendations for future work are as follows:

1. Statistical analyses of incidents on liquid transmission pipelines can be carried out to gain insights into main failure causes and failure modes. Furthermore, a comparative study can be carried out to evaluate the safety and reliability of transmission pipelines in comparison with other modes (such as rail) of transporting large quantities of liquid hydrocarbons.

2. The probability of ignition for ruptures of liquid transmission pipelines needs to be investigated. Furthermore, the probabilities of ignition for puncture of gas and liquid transmission pipelines should also be examined.

3. The failure consequences of transmission pipelines in terms of the property damage, environmental impact and business interruption can be studied based on the PHMSA incident data, which will provide crucial input for determining the optimal maintenance strategies for onshore pipelines.

Appendix A

Detailed Information of PHMSA Rupture Incidents for Developing the POI Model

Table A.1

RPTID	d /mm	p /MPa	MAOP /MPa	C_l	Ig.	RPTID	d /mm	p /MPa	MAOP /MPa	C_l	Ig.
20020026	660.4	4.6	5.2	2	Y	20080017	609.6	3.1	3.4	1	N
20020030	914.4	6.6	6.7	1	N	20080035	273.1	6.6	6.9	1	N
20020036	508.0	4.7	5.4	1	N	20080080	273.1	2.8	3.4	1	N
20020053	406.4	4.3	4.5	1	N	20080081	168.3	2.6	3.4	3	N
20020062	168.3	2.8	3.3	1	N	20080090	762.0	5.5	5.5	1	Y
20020069	762.0	5.2	6.5	1	Y	20080093	273.1	5.9	6.9	3	N
20020090	762.0	5.7	5.9	1	N	20080094	914.4	7.2	7.2	1	Y
20020091	273.1	4.4	6.1	1	N	20080095	609.6	5.7	6.2	1	N
20020096	762.0	4.9	7.1	1	N	20080143	355.6	6.8	6.9	1	N
20030001	406.4	2.4	2.6	3	N	20080146	323.9	2.7	3.1	1	N
20030002	273.1	2.4	3.4	1	N	20090010	168.3	11.7	12.4	1	N
20030005	914.4	5.8	5.8	1	Y	20090012	168.3	3.6	5.5	1	N
20030017	609.6	5.6	6.7	1	Y	20090022	323.9	4.6	6.9	3	N
20030020	168.3	6.2	7.4	3	N	20090023	406.4	6.6	7.2	3	Y
20030021	323.9	5.0	5.5	1	Y	20090030	609.6	5.4	5.5	1	N
20030022	406.4	5.6	5.7	1	Y	20090056	219.1	3.0	5.7	1	N
20030024	219.1	0.9	1.0	1	N	20090059	457.2	5.9	6.0	1	N
20030028	323.9	4.4	4.7	1	Y	20090061	609.6	5.4	5.5	1	Y
20030041	457.2	2.3	3.2	1	N	20090066	101.6	6.3	6.7	3	N
20030050	660.4	4.3	4.6	1	N	20090071	406.4	6.4	7.5	1	N
20030061	762.0	5.1	5.6	1	Y	20090075	508.0	4.0	4.5	1	N
20030065	762.0	6.4	6.9	1	Y	20090078	273.1	8.2	9.0	1	N
20030076	660.4	4.7	5.0	1	N	20090080	508.0	1.7	2.6	1	N
20030087	168.3	14.6	15.2	1	N	20090107	114.3	4.7	5.2	1	N
20030091	609.6	5.5	5.5	2	N	20090119	406.4	5.4	7.8	1	N
20030094	219.1	4.8	5.3	3	N	20090133	406.4	6.1	6.6	1	N
20030095	762.0	6.2	6.9	1	Y	20090135	323.9	2.9	3.4	1	N
20040004	660.4	4.3	4.5	1	Y	20090141	508.0	1.2	1.5	2	N
20040005	508.0	2.6	2.8	1	N	20100002	609.6	5.1	5.2	2	N
20040031	914.4	4.8	4.9	1	Y	20100012	406.4	4.4	5.0	1	N
20040032	114.3	4.1	4.5	1	N	20100013	406.4	5.4	6.2	1	N

20040035	406.4	5.4	5.5	1	Y	20100014	660.4	3.8	4.1	1	Y
20040053	168.3	7.3	7.5	1	N	20100050	914.4	6.6	7.2	1	N
20040072	323.9	5.1	6.6	1	N	20100051	219.1	3.6	4.0	1	N
20040086	508.0	4.6	4.6	1	N	20100068	508.0	2.0	2.0	1	N
20040104	508.0	4.0	7.1	1	N	20100070	762.0	2.7	2.8	3	Y
20040109	323.9	4.1	5.7	3	N	20100090	508.0	3.8	3.8	1	N
20040113	323.9	8.5	7.1	1	N	20100110	508.0	5.6	6.3	1	N
20040117	609.6	5.9	6.0	1	N	20110002	609.6	4.9	5.2	1	N
20050001	323.9	3.9	5.0	1	N	20110010	168.3	4.4	5.5	1	N
20050007	141.3	1.4	1.8	1	N	20110026	914.4	5.1	5.4	1	Y
20050008	127.0	3.1	4.2	1	N	20110038	508.0	1.0	7.2	1	N
20050009	219.1	1.6	3.4	1	N	20110202	508.0	3.7	4.0	1	N
20050011	508.0	2.2	8.4	1	N	20110231	323.9	2.4	3.4	2	N
20050015	219.1	6.5	9.9	1	Y	20110267	219.1	6.7	8.4	1	N
20050022	219.1	1.9	2.1	1	N	20110294	762.0	9.2	9.9	1	N
20050026	219.1	2.6	3.8	3	N	20110389	60.3	13.4	16.5	1	Y
20050036	863.6	4.4	5.3	1	Y	20110392	914.4	5.4	5.5	1	Y
20050049	558.8	3.0	3.1	1	N	20110393	914.4	5.2	5.4	1	Y
20050058	762.0	6.6	6.7	1	N	20120006	508.0	5.8	4.2	1	N
20050062	406.4	1.2	1.4	1	N	20120011	762.0	6.3	6.9	1	Y
20050065	914.4	5.7	5.9	1	Y	20120028	762.0	6.7	6.7	1	N
20050077	508.0	3.6	3.1	1	N	20120038	60.3	1.9	2.0	3	N
20050088	508.0	6.7	7.2	1	N	20120041	323.9	3.0	3.4	1	N
20050089	406.4	3.7	5.0	1	N	20120046	406.4	6.4	8.9	1	Y
20050122	273.1	1.5	2.6	3	N	20120055	406.4	4.4	6.6	1	Y
20050176	219.1	6.2	9.9	1	Y	20120056	406.4	7.8	6.9	1	Y
20060003	323.9	2.3	2.4	1	N	20120058	168.3	6.3	8.3	1	N
20060024	508.0	5.9	6.3	1	N	20120066	660.4	4.8	5.0	1	Y
20060048	33.4	2.8	3.1	2	N	20120086	273.1	8.6	9.5	1	Y
20060076	13.7	0.3	20.7	1	N	20120087	323.9	4.3	5.1	3	Y
20060077	219.1	3.0	3.0	1	N	20120099	406.4	6.6	6.9	1	N
20060079	323.9	2.1	2.3	-	N	20120100	406.4	7.2	6.9	1	Y
20060093	406.4	6.1	6.3	1	N	20120112	168.3	0.9	2.1	2	N
20060104	609.6	4.9	5.2	2	Y	20120123	219.1	5.2	5.4	1	N
20060121	323.9	4.2	5.6	1	N	20120128	406.4	3.3	4.2	1	Y
20060126	508.0	4.6	5.0	1	Y	20130001	508.0	6.4	6.9	2	Y
20060129	508.0	4.5	6.6	1	N	20130007	508.0	6.4	6.5	1	N
20060134	609.6	4.8	5.5	1	N	20130019	323.9	2.6	3.4	1	N
20070008	609.6	4.5	5.9	1	N	20130021	323.9	4.4	4.9	1	N
20070026	457.2	2.1	3.3	3	N	20130043	508.0	5.8	7.3	1	N

20070027	508.0	2.1	4.9	2	N	20130055	168.3	2.4	3.1	3	N
20070028	114.3	4.2	11.3	1	N	20130064	323.9	5.6	6.0	1	N
20070030	787.4	4.0	5.2	1	Y	20130066	762.0	6.6	6.7	1	Y
20070041	219.1	1.3	1.8	1	N	20130071	127.0	5.6	6.3	1	N
20070054	323.9	5.8	7.5	1	N	20130077	219.1	10.2	10.8	3	N
20070064	558.8	5.4	5.5	1	Y	20130081	323.9	5.6	6.9	1	N
20070066	273.1	5.5	6.7	1	N	20130084	219.1	5.5	6.5	1	N
20070074	323.9	2.3	3.2	1	N	20130088	323.9	7.7	8.3	1	Y
20070096	219.1	1.2	5.0	1	N	20130099	762.0	5.6	5.9	1	Y
20070097	508.0	7.5	7.4	1	Y	20130117	219.1	3.2	3.4	1	N
20070105	60.3	5.7	9.9	1	N	20130120	762.0	6.2	6.2	1	Y
20070108	406.4	3.2	5.0	1	N	20140015	660.4	4.0	4.1	1	Y
20070110	508.0	4.7	5.0	1	Y	20140017	323.9	1.5	3.0	1	N
20070116	219.1	5.4	5.8	1	N	20140037	219.1	5.2	5.5	3	N
20070123	609.6	5.3	5.5	1	N	20140042	457.2	4.5	4.8	1	Y
20070124	168.3	9.9	10.9	1	Y	20140049	508.0	6.5	6.6	1	N
20070129	323.9	10.1	11.5	1	Y	20140066	219.1	6.5	6.7	1	N
20070146	609.6	6.3	8.3	1	N	20140069	609.6	5.7	6.0	1	Y
20080001	762.0	6.2	6.2	1	Y	20140072	508.0	5.2	6.6	2	Y
20080003	762.0	6.4	6.4	1	Y	20140073	508.0	3.1	7.8	2	Y
20080006	609.6	4.2	4.5	1	N	20140082	219.1	5.3	9.1	1	N
20080008	508.0	5.9	6.9	1	N	20140106	558.8	5.6	5.9	1	N
20080013	406.4	6.6	7.1	2	Y	20140110	219.1	6.0	6.5	1	N

Note: RPTIP = Incident report ID; MAOP = Maximum allowable operating pressure; Ig = Ignition

Curriculum Vitae

Name:	Chio Lam
Post-secondary Education and Degrees:	Tsinghua University Beijing, China 2009-2013, Bachelor of Engineering (BEng) (Civil Engineering) The University of Western Ontario London, Ontario, Canada 2013-2015, Master of Engineering Science (MESc) (Structural Engineering)
Honours and Awards:	Western Graduate Research Scholarship (WGRS) 2013-2015 Graduate Student Teaching Assistantship 2013-2015
Related Work Experience:	Research and Teaching Assistant The University of Western Ontario 2013-2015